

This is the accepted manuscript made available via CHORUS. The article has been published as:

Effective field theory for large logarithms in radiative corrections to electron proton scattering

Richard J. Hill

Phys. Rev. D **95**, 013001 — Published 4 January 2017

DOI: [10.1103/PhysRevD.95.013001](https://doi.org/10.1103/PhysRevD.95.013001)

Effective field theory for large logarithms in radiative corrections to electron proton scattering

Richard J. Hill

TRIUMF, 4004 Wesbrook Mall, Vancouver, BC, V6T 2A3 Canada

Perimeter Institute for Theoretical Physics,

Waterloo, ON, N2L 2Y5 Canada and

The University of Chicago, Chicago, Illinois, 60637, USA

Abstract

Radiative corrections to elastic electron-proton scattering are analyzed in effective field theory. A new factorization formula identifies all sources of large logarithms in the limit of large momentum transfer, $Q^2 \gg m_e^2$. Explicit matching calculations are performed through two-loop order. A renormalization analysis in soft-collinear effective theory is performed to systematically compute and resum large logarithms. Implications for the extraction of charge radii and other observables from scattering data are discussed. The formalism may be applied to other lepton-nucleon scattering and e^+e^- annihilation processes.

PACS numbers: 13.40.Gp 06.20.Jr 14.20.Dh 12.20.Ds

I. INTRODUCTION

The 2010 measurement of the muonic hydrogen Lamb shift by the CREMA collaboration [1] determined a value of the proton electric charge radius, r_E , in serious ($\sim 7\sigma$) conflict with determinations from electronic hydrogen [2] and electron-proton scattering [3–5]. This “proton radius puzzle” has far reaching implications across particle, nuclear and atomic physics. Taken at face value, in the absence of explanations beyond the Standard Model, the muonic hydrogen measurement necessitates a $\gtrsim 5\sigma$ revision of the fundamental Rydberg constant, in addition to discarding or revising the predictions from a large body of previous results in both electron-proton scattering and hydrogen spectroscopy. Sources of systematic error that could be impacting electron-proton scattering measurements, such as incorrect form factor shape assumptions and inaccurate radiative corrections, are also at a numerically important level to impact neutrino-nucleus scattering, and hence the extraction of fundamental neutrino parameters, at current and future experiments.

A recent analysis of global electron-proton scattering data by the author with Lee and Arrington [6] obtained $r_E = 0.895(20)$ fm from the high statistics 2010 Mainz A1 dataset [7], and $r_E = 0.916(24)$ fm from other world data. A naive average of these results gives $r_E = 0.904(15)$ fm, significantly larger than the muonic hydrogen determination $r_E(\mu\text{H}) = 0.84087(39)$ fm. The analysis of Ref. [6] included a critical examination of experimental systematic errors and a rigorous treatment of theoretical uncertainty associated with form factor shape [8, 9]. When applied to the entire Q^2 range of the Mainz dataset, this treatment reinforces the anomaly with muonic hydrogen. However, the analysis also revealed a significant dependence of the extracted radius on the Q^2 range of data considered. As noted in this reference, standard models for radiative corrections were applied. These models use a phenomenological ansatz for treating logarithmically enhanced terms, $\sim \alpha^n \log^{2n}(Q^2/m_e^2)$, where $\log(Q^2/m_e^2) \approx 15$ for $Q^2 \sim \text{GeV}^2$. As shown here, such prescriptions fail to capture subleading logarithms beginning at order $\alpha^2 \log^3(Q^2/m_e^2)$.

More generally, a variety of conflicting conventions and implicit scheme choices are present in the literature for Born form factors, charge radii and radiative corrections. In this paper, the quantum field theoretical foundation for unambiguously defining these observables and quantifying uncertainties due to radiative corrections is constructed. A new factorization formula is derived that identifies all sources of large logarithms. The relation between

conflicting definitions of the charge radius and related observables in the literature is clarified. The formalism may be applied to a range of problems in lepton-hadron scattering and e^+e^- annihilation. The effective theory analysis simplifies and extends diagrammatic arguments for the cancellation and exponentiation of infrared singularities in QED [10].

The remainder of the paper is structured as follows. Section II analyzes the scattering problem when particle energies and masses are of comparable size. This analysis introduces the soft function that will apply identically to the more complicated relativistic case. Section III considers the relativistic case where new large logarithms appear. This analysis proceeds in stages, considering first the static limit of infinite target mass, then successively including recoil, structure, and nuclear charge corrections. The concluding Section IV summarizes the main results, discusses applications, and indicates directions for future work. Appendix A lists renormalization constants and conventions employed in the paper. Appendix B compares our preferred Born form factor convention to others in the literature. Appendix C lists relevant phase space integrals. Appendix D gives details of the computation of two-loop mixed real-virtual corrections in the static source limit. Appendix E presents the same computation using momentum regions analysis.

II. HEAVY PARTICLE

Consider the scattering of a fermion of mass M from a gauge source, in the regime of energy and momentum transfer $E \sim Q \sim M$, and including the effects of soft radiation of energy $\Delta E \ll M$. We will develop formalism that applies equally well to composite and elementary particles. For definiteness in the discussion we refer to the heavy particle as a “proton”.¹

The effective field theory separates physics at the hard scale, with particle virtualities $p^2 \sim M^2$, from physics at the soft scale, $p^2 \sim (\Delta E)^2$, and enables the resummation of large logarithms, $\log(M/\Delta E) \gg 1$ using renormalization group methods. We give a field-theoretic justification for the conventional separation between on-shell and Born form factors [6].

¹ To orient the reader: for the application to electron-proton scattering, the analysis of Section II can be viewed as describing the “lower vertex” (i.e., the proton) in single photon exchange approximation. Section III describes the “upper vertex” (i.e., the electron), before assembling both pieces and accounting for multiple photon exchange.

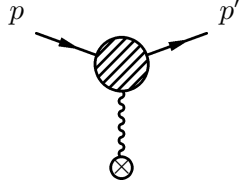


FIG. 1: Scattering of proton from electromagnetic source.

At the same time, we introduce formalism and notation that will carry over to the more complicated case of relativistic electron scattering (i.e., $Q^2 \gg m^2$) considered later.

A. Effective theory

For the process depicted in Fig. 1, introduce timelike unit vectors v^μ and v'^μ via

$$p^\mu = Mv^\mu, \quad p'^\mu = Mv'^\mu. \quad (1)$$

At factorization scale $\mu \sim M$, hard momentum modes are integrated out, leaving a low energy effective theory consisting of heavy particle source fields interacting with soft photons. The QED current is matched to an expansion in effective operators,

$$J^\mu = \bar{\psi}\gamma^\mu\psi \rightarrow \sum_i c_i(\mu, v \cdot v') \bar{h}_v \Gamma_i^\mu h_v, \quad (2)$$

where h_v , $h_{v'}$ denote heavy fermion fields satisfying $\not{v}h_v = h_v$.² The heavy fermion fields interact with soft photons, as described by the effective theory Lagrangian

$$\mathcal{L}_{\text{eff.}} = -\frac{1}{4}(F^{\mu\nu})^2 + \bar{h}_v(iv \cdot \partial + Ze v \cdot A)h_v + \bar{h}_{v'}(iv' \cdot \partial + Ze v' \cdot A)h_{v'} + \mathcal{O}(1/M), \quad (3)$$

where $Z = +1$ for the proton, A^μ is the electromagnetic field and $F_{\mu\nu} = \partial_\mu A_\nu - \partial_\nu A_\mu$.

² For reviews of heavy particle effective theories in the context of QCD and heavy quarks, see Refs. [11, 12]. NRQED was introduced in Ref. [13]. For a discussion of general heavy particle effective theories see Ref. [14].

B. One loop matching

An explicit basis of operator structures in Eq. (2) respecting the discrete symmetries of the electromagnetic current is

$$\Gamma_1^\mu = \gamma^\mu, \quad \Gamma_2^\mu = v^\mu + v'^\mu. \quad (4)$$

For an elementary particle, the matching may be performed perturbatively. In the $\overline{\text{MS}}$ scheme at renormalization scale μ , the matching coefficients are [15]

$$\begin{aligned} c_1(\mu, w) &= 1 - \frac{Z^2 \bar{\alpha}}{2\pi} \left[(wf(w) - 1) \log \frac{M^2}{\mu^2} - F(w) \right], \\ c_2(\mu, w) &= -\frac{Z^2 \bar{\alpha}}{4\pi} f(w), \end{aligned} \quad (5)$$

where $w \equiv v \cdot v'$,

$$\begin{aligned} f(w) &= \frac{1}{\sqrt{w^2 - 1}} \log(w_+), \\ F(w) &= \frac{w}{\sqrt{w^2 - 1}} \left[2\text{Li}_2(-w_-) + \frac{\pi^2}{6} + \frac{1}{2} \log^2(w_+) - \log(w_+) \log[2(w+1)] + \frac{3}{2} \log(w_+) \right] \\ &\quad + \frac{3}{2} f(w) - 2, \end{aligned} \quad (6)$$

and for a general quantity $a > 1$ we define

$$a_\pm \equiv a \pm \sqrt{a^2 - 1}. \quad (7)$$

The quantity $\bar{\alpha}$ denotes the running coupling in the $\overline{\text{MS}}$ scheme, $\bar{\alpha} \equiv \alpha(\mu)$.

The eikonal, $v \cdot A$, nature of the photon coupling in Eq. (3) implies that the soft photon matrix element is universal to the different operator structures Γ_i in Eq. (2). This universality becomes manifest with a Wilson line field redefinition,

$$h_v \rightarrow \mathcal{S}_v h_v, \quad \mathcal{S}_v(x) = \exp \left[iZe \int_{-\infty}^0 ds v \cdot A(x + sv) \right], \quad (8)$$

that isolates all photon dynamics in a soft-photon Wilson loop, $\mathcal{S}_v^\dagger \mathcal{S}_v$. The contribution of soft photons to the amplitude for the process depicted in Fig. 1 is independent of whether the particle is composite or elementary. We define the universal soft form factor to include appropriate wavefunction renormalization. Through one loop order this function reads,

$$F_S(w, \mu) = Z_h \left[\text{diagram 1} + \text{diagram 2} \right] = 1 - \frac{Z^2 \alpha}{2\pi} [wf(w) - 1] \log \frac{\mu^2}{\lambda^2}, \quad (9)$$

where λ is an infinitesimal photon mass acting as IR regulator, and Z_h is the onshell wave-function renormalization constant computed from the lagrangian (3) (cf. Appendix A). The complete (onshell, renormalized) amplitude for the process in Fig. 1 is conventionally expressed as

$$\langle J^\mu \rangle = \bar{u}_{v'} \left[\tilde{F}_1 \gamma^\mu + \tilde{F}_2 \frac{i}{2} \sigma^{\mu\nu} (v'_\nu - v_\nu) \right] u_v, \quad (10)$$

where $u_v = u(p)$ is a Dirac spinor and the onshell Dirac and Pauli form factors are

$$\begin{aligned} \tilde{F}_1(q^2) &= [c_1(w, \mu) + 2c_2(w, \mu)] F_S(w, \mu), \\ \tilde{F}_2(q^2) &= -2c_2(w, \mu) F_S(w, \mu), \end{aligned} \quad (11)$$

with $q^2 = -2M^2(w - 1)$. For a strongly interacting composite particle like the proton, perturbative matching is not possible. In this case, the Wilson coefficients $c_i(w, \mu)$ in Eq. (11) are identified as infrared finite “Born” form factors, to be extracted experimentally:

$$F_i(q^2)^{\text{Born}} \equiv \tilde{F}_i(q^2) F_S^{-1}(w, \mu = M), \quad (12)$$

where the choice $\mu = M$ is part of the Born convention. For a discussion of Born form factor extraction from experimental data, see Ref. [6]. A comparison to other conventions in the literature for Born form factors is given in Appendix B.

C. Resummation

To define an infrared finite observable, consider the process depicted in Fig. 1: scattering of a proton from an electromagnetic source, allowing radiation of energy $\Delta E \ll M$. Suppressing a kinematic prefactor, the cross section is governed by the factorization formula,

$$d\sigma \propto H \left(\frac{M}{\mu}, v \cdot v' \right) S \left(\frac{\Delta E}{\mu}, v \cdot v', v^0, v'^0 \right). \quad (13)$$

The hard function is

$$H = \sum_{i,j} c_i(\mu) c_j^*(\mu) \text{Tr} \left(\Gamma_i \frac{1 + \not{p}}{2} \bar{\Gamma}_j \frac{1 + \not{p}'}{2} \right). \quad (14)$$

The soft function may be expanded according to photon number,

$$S = S_{0\gamma} + S_{1\gamma} + S_{2\gamma} + \dots, \quad (15)$$

and for each contribution we may expand as a series in α ,

$$S_{n\gamma} = \sum_{i=n}^{\infty} \left(\frac{\bar{\alpha}}{4\pi} \right)^i S_{n\gamma}^{(i)}. \quad (16)$$

Neglecting real photon emission,

$$S_{0\gamma} = S(\Delta E = 0) = |F_S|^2, \quad (17)$$

where F_S is the universal soft form factor, whose one-loop expansion is given in Eq. (9).

From the Feynman rules of the lagrangian (3), the first order real photon correction is

$$\begin{aligned} S_{1\gamma}^{(1)} &= -(4\pi Z)^2 \int_{\ell^0 \leq \Delta E} \frac{d^3\ell}{(2\pi)^3} \frac{1}{2\ell^0} \left(\frac{v^\mu}{v \cdot \ell} - \frac{v'^\mu}{v' \cdot \ell} \right)^2 \\ &= 4Z^2 \left\{ 2 \log \left(\frac{2\Delta E}{\lambda} \right) [wf(w) - 1] + G(w, v^0, v'^0) \right\}, \end{aligned} \quad (18)$$

where $\ell^0 = \sqrt{\vec{\ell}^2 + \lambda^2}$, and

$$\begin{aligned} G(w, v^0, v'^0) &= \frac{v^0}{\sqrt{(v^0)^2 - 1}} \log v_+^0 + \frac{v'^0}{\sqrt{(v'^0)^2 - 1}} \log v_+'^0 + \frac{w}{\sqrt{w^2 - 1}} \left[\log^2(v_+^0) - \log^2(v_+'^0) \right] \\ &+ \text{Li}_2 \left(1 - \frac{v_+^0}{\sqrt{w^2 - 1}} (w_+ v^0 - v'^0) \right) + \text{Li}_2 \left(1 - \frac{v_-^0}{\sqrt{w^2 - 1}} (w_+ v^0 - v'^0) \right) \\ &- \text{Li}_2 \left(1 - \frac{v_+'^0}{\sqrt{w^2 - 1}} (v^0 - w_- v'^0) \right) - \text{Li}_2 \left(1 - \frac{v_-'^0}{\sqrt{w^2 - 1}} (v^0 - w_- v'^0) \right) \Big]. \end{aligned} \quad (19)$$

The quantities v_\pm^0 , v'_\pm^0 , w_\pm are defined by Eq. (7). The total first order correction is thus

$$S^{(1)} = Z^2 \left\{ 8 \log \left(\frac{2\Delta E}{\mu} \right) [wf(w) - 1] + 4G(w, v^0, v'^0) \right\}. \quad (20)$$

When $\Delta E \ll M$, large logarithms are present regardless of the choice for factorization scale μ in Eq. (13). This is seen explicitly in the one-loop corrections for the hard function in Eqs. (5) and (14), and for the soft function in Eq. (20). The following renormalization analysis systematically resums large logarithms to all orders in perturbation theory.

The anomalous dimension of the effective operators (2) relates the renormalization of the hard function to the cusp anomalous dimension for QED [16, 17], (cf. Appendix A)

$$\frac{d}{d \log \mu} H(\mu) = 2\Gamma_{\text{cusp}}(w) H(\mu). \quad (21)$$

Expanding in α ,

$$\Gamma_{\text{cusp}}(w) = \sum_{n=0}^{\infty} \left(\frac{\bar{\alpha}}{4\pi} \right)^{n+1} \Gamma_n^{\text{cusp}}(w), \quad (22)$$

where the leading terms are (cf. Appendix A)

$$\Gamma_0^{\text{cusp}}(w) = 4[wf(w) - 1], \quad \Gamma_1^{\text{cusp}}(w) = -\frac{20}{9}n_f\Gamma_0^{\text{cusp}}. \quad (23)$$

Here n_f denotes the number of light fermions in the effective theory. In this example, we take the muon mass, proton mass and other hadronic scales as large compared to ΔE , and work with $n_f = 1$ in the regime with formal power counting $m = m_e \sim \Delta E \ll E \sim m_\mu \sim m_p = M$.³ Solution of Eq. (21) then yields

$$\begin{aligned} \frac{H(\mu_H)}{H(\mu_L)} &= \frac{S(\mu_L)}{S(\mu_H)} \\ &= \exp \left\{ -\frac{\Gamma_0^{\text{cusp}}(w)}{\beta_0} \left[\log \frac{\alpha(\mu_H)}{\alpha(\mu_L)} + \frac{1}{4\pi} \left(\frac{\Gamma_1^{\text{cusp}}}{\Gamma_0^{\text{cusp}}} - \frac{\beta_1}{\beta_0} \right) (\alpha(\mu_H) - \alpha(\mu_L)) + \dots \right] \right\} \\ &= \exp \left\{ 4[wf(w) - 1] \left[\frac{\alpha}{4\pi} \log \frac{\mu_H^2}{\mu_L^2} + \left(\frac{\alpha}{4\pi} \right)^2 \left(\frac{2}{3} \log^2 \frac{\mu_H^2}{\mu_L^2} + \frac{4}{3} \log \frac{\mu_H^2}{\mu_L^2} \log \frac{\mu_L^2}{m^2} \right. \right. \right. \\ &\quad \left. \left. \left. - \frac{20}{9} \log \frac{\mu_H^2}{\mu_L^2} \right) + \mathcal{O}(\alpha^3) \right] \right\}, \end{aligned} \quad (24)$$

where the result in the last line is expressed in terms of the low energy, onshell, fine structure constant α .

To connect with observables such as the Born form factors (12) defined at $\mu \sim M$, we may expand soft functions in perturbation theory at the scale $\mu_L \sim \Delta E \sim m$, where no large logarithms appear, as in Eq. (20). We may then use Eq. (24) to evaluate the soft function appearing in Eq. (12) at $\mu_H \sim M$, systematically controlling large logarithms.

We remark that a simple exponentiation ansatz,

$$S \rightarrow \exp \left[\frac{\alpha}{4\pi} S^{(1)} \right], \quad (25)$$

fails to capture logarithmically enhanced terms beginning at order $\alpha^2 \log^2[M^2/(\Delta E)^2]$. Such terms are below typical experimental accuracies for $w = \mathcal{O}(1)$. However, at large recoil, $w \gg 1$, additional factors involving large logarithms, $\log(w)$, appear. We turn now to this case, where control of logarithmically enhanced corrections beyond first order in α is essential.

³ It is straightforward to include perturbative corrections due to the muon.

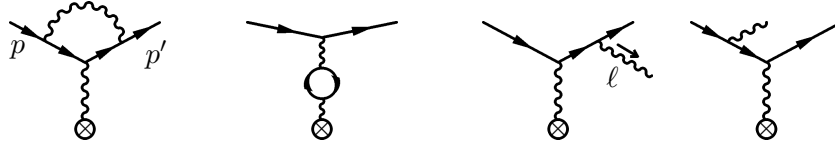


FIG. 2: First order radiative corrections to electron scattering from static source.

III. RELATIVISTIC PARTICLE

When particle velocities satisfy $v \cdot v' \gg 1$, new large logarithms appear in perturbation theory which are not resummed by the renormalization analysis in the heavy particle effective theory of the previous section. For example, $c_i(\mu, v \cdot v')$ in Eq. (5) contains large logarithms, $\log(v \cdot v')$, regardless of the choice for factorization scale μ . In order to isolate and resum these additional large logarithms, we must extend the effective theory to include collinear degrees of freedom [18–25]. Before turning to the effective theory description, let us examine the explicit two-loop calculation for relativistic electron-proton scattering in the static source limit. We will then perform the effective theory analysis in this limit before including arbitrary recoil corrections, and radiative corrections involving the proton.

A. Two loop corrections in static limit

To isolate the essential points, let us consider the problem of relativistic unpolarized electron-proton scattering in the static-source limit of large proton mass: $m \ll E \ll M$, where m and M denote the electron and proton masses and E is the electron energy. Neglecting power corrections in m/E , and working to first order in nuclear charge (i.e., single photon exchange), the cross section may be written

$$d\sigma = \frac{(d\sigma)_{\text{Mott}}}{[1 - \hat{\Pi}(q^2)]^2} (1 + \delta_e + \delta_{e\gamma} + \delta_{e\gamma\gamma} + \dots) \equiv \frac{(d\sigma)_{\text{Mott}}}{[1 - \hat{\Pi}(q^2)]^2} (1 + \delta). \quad (26)$$

Here $(d\sigma/d\Omega)_{\text{Mott}} = \alpha^2 \cos^2(\theta/2)/[4E^2 \sin^4(\theta/2)]$ is the tree-level, Mott, cross section in terms of the angle θ between initial and final electron directions in the lab frame, $\hat{\Pi}(q^2)$ is the photon vacuum polarization function, and δ is the total radiative correction. For numerical evaluations we employ the onshell coupling, $\alpha = 1/137.036$. Each term δ_X in Eq. (26) corresponds to different numbers of final state photons and is expanded according to $\delta_X = \sum_{n=0}^{\infty} \left(\frac{\alpha}{4\pi}\right)^n \delta_X^{(n)}$.

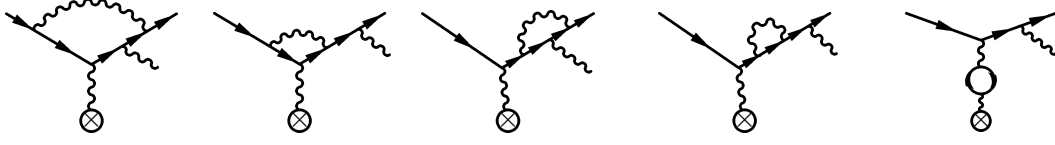


FIG. 3: Second order radiative corrections to electron scattering from static source. Diagrams involving photon emission from the initial state electron are not shown.

Consider radiative corrections at first order in α , cf. Fig. 2. Regulating infrared divergences with an infinitesimal photon mass λ , corrections with just an electron in the final state are

$$1 + \delta_e = [F_1(q^2, m^2, \lambda^2)]^2, \quad F_1 = 1 + \sum_{n=1}^{\infty} \left(\frac{\alpha}{4\pi}\right)^n F_1^{(n)}, \quad (27)$$

where F_1 is the Dirac form factor of the electron. At large spacelike momentum transfer $Q^2 = -q^2 \gg m^2$, the limit of Eq. (11), using Eqs. (5) and (9), yields [$L \equiv \log(Q^2/m^2)$]

$$F_1^{(1)} = 4 \log \frac{\lambda}{m} (L - 1) - L^2 + 3L - 4 + \frac{\pi^2}{3}. \quad (28)$$

Real radiation corrections are given by the limit of Eq. (18),

$$\delta_{e\gamma}^{(1)} = -8 \left(\log \frac{E}{\Delta E} + \log \frac{\lambda}{m} \right) (L - 1) + 2L^2 + 4\text{Li}_2 \left(\cos^2 \frac{\theta}{2} \right) - \frac{4\pi^2}{3}, \quad (29)$$

where a cut $\ell^0 \leq \Delta E \ll E$ is placed on photon energy. The total first order correction, $\delta^{(1)} = \delta_e^{(1)} + \delta_{e\gamma}^{(1)}$, is infrared finite.

Second order corrections containing two-photon final states (“double bremsstrahlung”) are

$$\begin{aligned} \delta_{e\gamma\gamma}^{(2)} &= \frac{1}{2!} \int_{\Delta E} \frac{d^3\ell}{\pi\ell^0} \frac{d^3\ell'}{\pi\ell'^0} \left(\frac{Q^2}{p \cdot \ell p' \cdot \ell} - \frac{m^2}{(p \cdot \ell)^2} - \frac{m^2}{(p' \cdot \ell)^2} \right) \left(\frac{Q^2}{p \cdot \ell' p' \cdot \ell'} - \frac{m^2}{(p \cdot \ell')^2} - \frac{m^2}{(p' \cdot \ell')^2} \right) \\ &= \frac{1}{2!} [\delta_{e\gamma}^{(1)}]^2 - \frac{16\pi^2}{3} (L - 1)^2, \end{aligned} \quad (30)$$

where a cut $\ell^0 + \ell'^0 \leq \Delta E$ is placed on photon energy. Contributions to second order mixed real-virtual corrections are displayed in Fig. 3. The computation of these contributions is described in Appendix D. After renormalization, and neglecting power suppressed contributions, the result takes the simple form

$$\delta_{e\gamma}^{(2)} = \delta_e^{(1)} \delta_{e\gamma}^{(1)}, \quad (31)$$

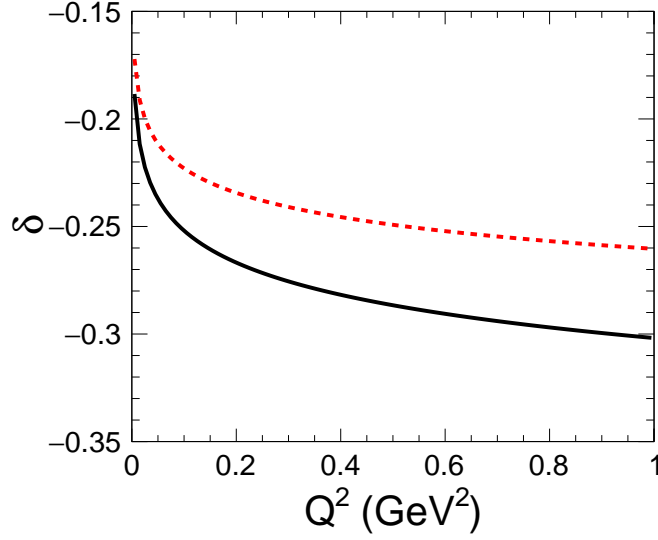


FIG. 4: Radiative correction δ from Eq. (26), in static source limit for $E = 1$ GeV, $\Delta E = 5$ MeV, computed at first (bottom, blue, curve) and second (top, red, curve) in α .

where $\delta_e^{(1)} = 2F_1^{(1)}$ in Eq. (28) and $\delta_{e\gamma}^{(1)}$ is given in Eq. (29). Finally, second order virtual corrections, $\delta_e^{(2)}$, are given by expanding Eq. (27) [26–28]. The complete second order correction may be written

$$\delta^{(2)} = \frac{1}{2!}[\delta^{(1)}]^2 - \frac{8}{9}L^3 + \left(\frac{76}{9} - \frac{16\pi^2}{3}\right)L^2 + \left(-\frac{979}{27} + \frac{52\pi^2}{9} + 48\zeta(3)\right)L + \frac{4252}{27} + \frac{31\pi^2}{3} - 16\pi^2 \log 2 - 72\zeta(3) - \frac{64\pi^4}{45}. \quad (32)$$

Fig. 4 displays the total correction δ in Eq. (26) at first and second order in perturbation theory, for illustrative values $E = 1$ GeV, $\Delta E = 5$ MeV, and physical electron mass. Recall that these results are in the formal static source limit, $E \ll M$. Logarithmically enhanced corrections beginning at order $\alpha^2 L^3$ are not captured by a simple exponentiation ansatz, $\delta \rightarrow \exp[\frac{\alpha}{4\pi}\delta^{(1)}]$. In the next section we derive the effective theory that allows identification and resummation of large logarithms.

B. Effective theory: matching

To determine the origin of the different contributions in Eq. (32), and to systematically resum large logarithms in perturbation theory, let us construct an effective theory to separate

the physics at different energy scales. We focus on the formal counting $m \sim \Delta E$ and $Q \sim E \gg m$ (i.e., $v \cdot v' \gg 1$). Appendix E outlines an effective operator analysis analogous to Eqs. (2) and (3). In place of Eq. (13), the new factorization formula, valid up to $\mathcal{O}(m^2/Q^2)$ corrections and verified explicitly through two-loop order (cf. Appendices D and E), reads

$$d\sigma \propto H\left(\frac{Q^2}{\mu^2}\right) J\left(\frac{m^2}{\mu^2}\right) R\left(\frac{m^2}{\mu^2}, \frac{p \cdot p'}{m^2}\right) S\left(\frac{\Delta E}{\mu}, \frac{p \cdot p'}{m^2}, \frac{E}{m}, \frac{E'}{m}\right). \quad (33)$$

The explicit matching with QED is most easily performed using dimensional regularization, where dimensionful but scaleless integrals vanish. The (bare, unrenormalized) hard function is then $[4\pi\alpha_{\text{bare}} \equiv e_{\text{bare}}^2(4\pi)^\epsilon e^{-\gamma_E \epsilon}]$

$$\sqrt{H^{\text{bare}}} \equiv F_H^{\text{bare}} = F_1(q^2, m^2 = 0, \lambda^2 = 0) = 1 + \sum_{i=1}^{\infty} \left(\frac{\alpha_{\text{bare}} Q^{-2\epsilon}}{4\pi} \right)^i F_{Hi}^{\text{bare}}, \quad (34)$$

where results for $F_1(q^2, 0, 0)$ through two-loop order are [29, 30],⁴

$$\begin{aligned} F_{H1}^{\text{bare}} &= -\frac{2}{\epsilon^2} - \frac{3}{\epsilon} - 8 + \zeta_2 + \epsilon \left(-16 + \frac{\pi^2}{4} + \frac{14}{3}\zeta_3 \right) + \epsilon^2 \left(-32 + \frac{2\pi^2}{3} + 7\zeta_3 + \frac{47}{720}\pi^4 \right) + \mathcal{O}(\epsilon^3), \\ F_{H2}^{\text{bare}} &= \frac{2}{\epsilon^4} + \frac{6}{\epsilon^3} + \frac{1}{\epsilon^2} \left(\frac{41}{2} - 2\zeta_2 \right) + \frac{1}{\epsilon} \left(\frac{221}{4} - \frac{64}{3}\zeta_3 \right) + \frac{1151}{8} + \frac{17}{2}\zeta_2 - 58\zeta_3 - 13\zeta_2^2 \\ &\quad + 2n_f \left[\frac{1}{3\epsilon^3} + \frac{14}{9\epsilon^2} + \frac{1}{\epsilon} \left(\frac{353}{54} + \frac{\zeta_2}{3} \right) + \frac{7541}{324} + \frac{14\zeta_2}{9} - \frac{26\zeta_3}{9} \right] + \mathcal{O}(\epsilon). \end{aligned} \quad (35)$$

In the $\overline{\text{MS}}$ scheme, we define (at $n_f = 1$)

$$F_H(\mu) = Z_H F_H^{\text{bare}}, \quad (36)$$

with the renormalization constant,

$$\begin{aligned} Z_H &= 1 + \frac{\bar{\alpha}}{4\pi} \left[\frac{2}{\epsilon^2} + \frac{1}{\epsilon} \left(-2 \log \frac{Q^2}{\mu^2} + 3 \right) \right] + \left(\frac{\bar{\alpha}}{4\pi} \right)^2 \left[\frac{2}{\epsilon^4} + \frac{1}{\epsilon^3} \left(-4 \log \frac{Q^2}{\mu^2} + 8 \right) \right. \\ &\quad \left. + \frac{1}{\epsilon^2} \left(2 \log^2 \frac{Q^2}{\mu^2} - \frac{22}{3} \log \frac{Q^2}{\mu^2} + \frac{97}{18} \right) + \frac{1}{\epsilon} \left(\frac{20}{9} \log \frac{Q^2}{\mu^2} - \frac{179}{108} - \frac{4\pi^2}{3} + 12\zeta_3 \right) \right] + \mathcal{O}(\alpha^3). \end{aligned} \quad (37)$$

The explicit renormalized hard function is

$$F_H(\mu) = 1 + \frac{\bar{\alpha}}{4\pi} \left[-\log^2 \frac{Q^2}{\mu^2} + 3 \log \frac{Q^2}{\mu^2} - 8 + \frac{\pi^2}{6} \right]$$

⁴ There is a transcription error in the $\mathcal{O}(\epsilon^2)$ coefficient in Eq. (15) of Ref. [30]: $-47\pi^4/2880$ should be replaced by $+47\pi^4/2880$, in accordance with Eq. (17) of the same reference [31].

$$\begin{aligned}
& + \left(\frac{\bar{\alpha}}{4\pi}\right)^2 \left[\frac{1}{2} \log^4 \frac{Q^2}{\mu^2} - \frac{31}{9} \log^3 \frac{Q^2}{\mu^2} + \left(\frac{301}{18} - \frac{\pi^2}{6}\right) \log^2 \frac{Q^2}{\mu^2} \right. \\
& + \left. \left(-\frac{2051}{54} - \frac{35\pi^2}{18} + 24\zeta_3\right) \log \frac{Q^2}{\mu^2} + \frac{235\pi^2}{54} - \frac{266\zeta_3}{9} + \frac{36995}{648} - \frac{83\pi^4}{360} \right] + \mathcal{O}(\alpha^3),
\end{aligned} \tag{38}$$

where $\bar{\alpha} = \alpha(\mu)$ is the $\overline{\text{MS}}$ QED coupling with $n_f = 1$ at renormalization scale μ (for a summary of renormalization constants and conventions see Appendix A).

The soft function in Eq. (33) is the same function of its arguments as the soft function in Eq. (13). For virtual corrections this function⁵ becomes trivial ($S = 1$) in dimensional regularization at $\lambda = 0$ (the relevant integrals are dimensionful but scaleless). The product of the (bare, unrenormalized) jet and remainder functions (defined separately below) is thus

$$\sqrt{(JR)^{\text{bare}}} = F_{JR}^{\text{bare}} = \frac{F_1(q^2, m^2, \lambda^2 = 0)}{F_1(q^2, m^2 = 0, \lambda^2 = 0)} = 1 + \sum_{i=1}^{\infty} \left(\frac{\alpha_{\text{bare}} m^{-2\epsilon}}{4\pi} \right)^i F_{JRi}^{\text{bare}}, \tag{39}$$

where results for $F_1(q^2, m^2, 0)$ through two-loop order are given in Refs. [32, 33]. These results imply [34], (now at $n_f = 1$)

$$\begin{aligned}
F_{JR1}^{\text{bare}} &= \frac{2}{\epsilon^2} + \frac{1}{\epsilon} + \frac{\pi^2}{6} + 4 + \epsilon \left(8 + \frac{\pi^2}{12} - \frac{2\zeta_3}{3} \right) + \epsilon^2 \left(16 - \frac{\zeta_3}{3} + \frac{\pi^4}{80} + \frac{\pi^2}{3} \right) + \mathcal{O}(\epsilon^3), \\
F_{JR2}^{\text{bare}} &= \frac{2}{\epsilon^4} + \frac{4}{3\epsilon^3} + \frac{1}{\epsilon^2} \left(\frac{145}{18} + \frac{\pi^2}{3} \right) + \frac{1}{\epsilon} \left(\frac{1405}{108} - \frac{11\pi^2}{9} + \frac{32\zeta_3}{3} \right) + \frac{58957}{648} + \frac{397\pi^2}{108} - \frac{62\zeta_3}{9} \\
& - 8\pi^2 \log 2 - \frac{77\pi^4}{180} + \log \frac{Q^2}{m^2} \left(-\frac{4}{3\epsilon^2} + \frac{20}{9\epsilon} - \frac{112}{27} - \frac{2\pi^2}{9} \right) + \mathcal{O}(\epsilon).
\end{aligned} \tag{40}$$

The product $F_H F_{JR}$ represents the matching coefficient onto the soft operator after integrating out the electron mass scale. In the $\overline{\text{MS}}$ scheme for the $n_f = 0$ theory, we write

$$F_S(\mu) = Z_S^{-1} F_S^{\text{bare}}. \tag{41}$$

From the divergent terms in $F_H F_{JR}$ we may read off

$$Z_S = 1 + \frac{\bar{\alpha}_0}{4\pi} \frac{2}{\epsilon} \left(-\log \frac{Q^2}{m^2} + 1 \right) + \left(\frac{\bar{\alpha}_0}{4\pi} \right)^2 \frac{2}{\epsilon^2} \left(-\log \frac{Q^2}{m^2} + 1 \right)^2 + \mathcal{O}(\alpha^3), \tag{42}$$

with $\bar{\alpha}_0 = \alpha_0(\mu)$ the $\overline{\text{MS}}$ coupling with $n_f = 0$ (in $d = 4$ dimensions, $\bar{\alpha}_0$ reduces to the onshell α). The product of renormalized jet and remainder functions is given by

$$F_{JR}(\mu) = Z_H^{-1} Z_S F_{JR}^{\text{bare}}$$

⁵ The (infrared-divergent) soft function including only virtual corrections is $S(\Delta E = 0) = |F_S|^2$, cf. Eq. (44).

$$\begin{aligned}
&= 1 + \frac{\bar{\alpha}_1(\mu)}{4\pi} \left(\log^2 \frac{m^2}{\mu^2} - \log \frac{m^2}{\mu^2} + 4 + \frac{\pi^2}{6} \right) \\
&\quad + \left(\frac{\bar{\alpha}_1(\mu)}{4\pi} \right)^2 \left[\log \frac{Q^2}{m^2} \left(-\frac{4}{3} \log^2 \frac{m^2}{\mu^2} - \frac{40}{9} \log \frac{m^2}{\mu^2} - \frac{112}{27} \right) + \frac{1}{2} \log^4 \frac{m^2}{\mu^2} \right. \\
&\quad - \frac{5}{9} \log^3 \frac{m^2}{\mu^2} + \log^2 \frac{m^2}{\mu^2} \left(\frac{53}{18} + \frac{\pi^2}{6} \right) + \log \frac{m^2}{\mu^2} \left(\frac{251}{54} + \frac{49\pi^2}{18} - 24\zeta_3 \right) \\
&\quad \left. - 8\pi^2 \log 2 + \frac{76\pi^2}{27} - \frac{163\pi^4}{360} - \frac{58\zeta_3}{9} + \frac{39949}{648} \right] + \mathcal{O}(\alpha^3). \tag{43}
\end{aligned}$$

The remaining (bare, unrenormalized) soft function for virtual corrections with nonvanishing λ is

$$\sqrt{S(\Delta E = 0)^{\text{bare}}} \equiv F_S^{\text{bare}} = \frac{F_1(q^2, m^2, \lambda^2)}{F_1(q^2, m^2, \lambda^2 = 0)}, \tag{44}$$

where results for $F_1(q^2, m^2, \lambda^2)$ through two-loop order are given in Refs. [27, 28]. The renormalized soft function is given by Eq. (41), or equivalently,

$$\begin{aligned}
F_S(\mu) &= \frac{F_1(q^2, m^2, \lambda^2)}{F_H(\mu)F_{JR}(\mu)} \\
&= 1 + \frac{\bar{\alpha}_0}{4\pi} \left[2 \log \frac{\lambda^2}{\mu^2} \left(\log \frac{Q^2}{m^2} - 1 \right) \right] + \left(\frac{\bar{\alpha}_0}{4\pi} \right)^2 \left[2 \log^2 \frac{\lambda^2}{\mu^2} \left(\log \frac{Q^2}{m^2} - 1 \right)^2 \right] + \mathcal{O}(\alpha^3). \tag{45}
\end{aligned}$$

C. Factorization of jet and remainder function

Inspection of the explicit matching results in Eqs. (38), (43), and (45) reveals a pattern of large logarithms. $H(\mu)$ is free of large logarithms provided $\mu \sim Q$. $S(\mu)$ contains large logarithms irrespective of the choice of μ , but in an exponentiated form. The product $(JR)(\mu)$ is free of large logarithms through one loop order provided $\mu \sim m$, but contains large logarithms at two-loop order.

Note that the combinations H , JR and S are given by the simple momentum regions analysis encoded by the form factor combinations in Eqs. (34), (39) and (44), respectively. In particular, the hard function H is given by hard loop momenta with all components of order the hard scale Q . The soft function S is given by soft loop momenta with all components of order λ (i.e., small compared to other scales). The product JR , whose decomposition we now discuss, arises from the remaining momentum regions where loop momenta are collinear to one of the external particles. The nontrivial overlap of soft and collinear regions (and

the associated subtractions, cf. Appendix E) manifests itself as residual, non-factorized, large logarithms, cf. Eq. (43). Such large logarithms have been studied in a variety of frameworks for applications involving massless fermions [36–38].⁶ The presence of a fermion mass m provides a physical cutoff in the collinear integrals, and we proceed as follows to isolate the large logarithms and provide an operator definition of separate “jet” (J) and “remainder” (R) functions. This factorization of the JR function is obtained by considering an intermediate theory in which the electron is dynamical inside closed loops, but where the valence electron is treated as a heavy particle field. The R function is then given by matching the soft operator defined in a theory with a dynamical fermion of mass m , to the soft operator defined in a theory without dynamical fermion.⁷ We find

$$\sqrt{R^{\text{bare}}} = F_R^{\text{bare}} = 1 + \left(\frac{\alpha_{\text{bare}} m^{-2\epsilon}}{4\pi} \right)^2 \left[\log \frac{Q^2}{m^2} \left(-\frac{4}{3\epsilon^2} + \frac{20}{9\epsilon} - \frac{112}{27} - \frac{2\pi^2}{9} \right) + \frac{2}{\epsilon^2} - \frac{8}{3\epsilon} + \frac{\pi^2}{3} + \frac{52}{9} \right] + \mathcal{O}(\alpha^3), \quad (46)$$

where the result includes the two-loop vertex correction with closed fermion loop [34], as well as a contribution from wavefunction renormalization in the massive fermion theory [35].⁸ After renormalization,

$$\begin{aligned} F_R(\mu) &= Z_S Z_{S,n_f=1}^{-1} F_R^{\text{bare}} \\ &= 1 + \left(\frac{\bar{\alpha}_1(\mu)}{4\pi} \right)^2 \left[\log \frac{Q^2}{m^2} \left(-\frac{4}{3} \log^2 \frac{m^2}{\mu^2} - \frac{40}{9} \log \frac{m^2}{\mu^2} - \frac{112}{27} \right) + \frac{8}{3} \log^2 \frac{m^2}{\mu^2} + \frac{16}{3} \log \frac{m^2}{\mu^2} + \frac{\pi^2}{9} + \frac{52}{9} \right] + \mathcal{O}(\alpha^3). \end{aligned} \quad (47)$$

Having factored out $R(\mu)$, the remaining $J(\mu)$ is given by

$$\begin{aligned} \sqrt{J(\mu)} &= F_J(\mu) \\ &= 1 + \frac{\bar{\alpha}_1(\mu)}{4\pi} \left(\log^2 \frac{m^2}{\mu^2} - \log \frac{m^2}{\mu^2} + 4 + \frac{\pi^2}{6} \right) + \left(\frac{\bar{\alpha}_1(\mu)}{4\pi} \right)^2 \left[\frac{1}{2} \log^4 \frac{m^2}{\mu^2} - \frac{5}{9} \log^3 \frac{m^2}{\mu^2} + \log^2 \frac{m^2}{\mu^2} \left(\frac{5}{18} + \frac{\pi^2}{6} \right) + \log \frac{m^2}{\mu^2} \left(-\frac{37}{54} + \frac{49\pi^2}{18} - 24\zeta_3 \right) - 8\pi^2 \log 2 + \frac{73\pi^2}{27} - \frac{163\pi^4}{360} \right] \end{aligned}$$

⁶ Reference [36] considers the massive fermion case through one loop order.

⁷ Recall [see Eq. (8)] that the soft operator is defined in terms of the Wilson loop of soft photons, $\sqrt{S} = \langle S_v^\dagger S_v \rangle$.

⁸ This operator definition of F_R differs from the quantity δS in Ref. [34] by inclusion of onshell renormalization factors. The jet function F_J in Eq. (48) correspondingly differs from the quantity Z_J in Ref. [34].

$$-\frac{58\zeta_3}{9} + \frac{36205}{648} \Big] + \mathcal{O}(\alpha^3). \quad (48)$$

Although the impact of $R(\mu)$ is numerically small, it is interesting from a formal perspective to understand the all orders structure of large logarithms appearing in this function. The operator definition identifying $R(\mu)$ as a ratio of Wilson loop matrix elements in $n_f = 1$ and $n_f = 0$ can be used to show that $\log R(\mu)$ contains only a single power of the large logarithm, $\log(Q^2/m^2)$, to all orders in perturbation theory [16].⁹ This ensures that high powers of large logarithms do not upset the power counting of the resummed perturbative expansion.

D. Soft-collinear factorization for real radiation

Factorization of the soft function in Eq. (33) from the remaining process is nontrivial. It can be shown [cf. Eq. (D8)] that multiple low-energy regions contribute to the physical matrix element. This complicates a simple eikonal decoupling argument like Eq. (8) that applies in the heavy-particle case. Through two-loop order, factorization is equivalent to the vanishing of additional contributions on the right hand side of Eq. (31). Direct evaluation of such contributions is performed in the full theory in Appendix D, and in the effective theory in Appendix E.

E. Two-loop soft function

Having derived the functions $H(\mu)$, $J(\mu)$ and $R(\mu)$, and having demonstrated soft-collinear factorization for real radiation, let us specify the remaining soft function through two-loop order. The complete soft function including real radiation, $S(\Delta E)$ in Eq. (33), is obtained from Feynman diagrams with only soft photons, cf. Figs. 8 and 9. Our definition ensures that this function is identical to the soft function appearing in Eq. (13), extended to general $v \cdot v' \gg 1$.¹⁰ Using the explicit results (45) and (30), and the soft contribution to

⁹ In particular, $d \log R(\mu)/d \log \mu$ is given by the difference of cusp anomalous dimensions with $n_f = 1$ and $n_f = 0$, cf. Eqs. (21), (22), and (23).

¹⁰ Note that with this definition, closed electron loop corrections are defined to be contained in R .

Eq. (31), the complete corrections at one and two-loop order are¹¹

$$\begin{aligned} S^{(1)} &= -4 \left(\log \frac{\mu^2}{m^2} + \log \frac{E^2}{(\Delta E)^2} \right) (L-1) + 2L^2 + 4\text{Li}_2 \left(\cos^2 \frac{\theta}{2} \right) - \frac{4\pi^2}{3}, \\ S^{(2)} &= \frac{1}{2!} [S^{(1)}]^2 - \frac{16\pi^2}{3} (L-1)^2. \end{aligned} \quad (49)$$

F. Effective theory: resummation

After renormalization in the $\overline{\text{MS}}$ scheme at scale μ , the hard function is free of large logarithms provided that the matching scale satisfies $\mu_H \sim Q$. Evolution to low scales $\mu_L \sim m$ is governed by (cf. Appendix A)

$$\frac{d \log H}{d \log \mu} = 2 \left[\gamma_{\text{cusp}}(\alpha) \log \frac{Q^2}{\mu^2} + \gamma(\alpha) \right]. \quad (50)$$

The cusp anomalous dimension for massless QED ($n_f = 1$) reads

$$\gamma_{\text{cusp}} = \sum_{n=0}^{\infty} \left(\frac{\bar{\alpha}}{4\pi} \right)^{n+1} \gamma_n^{\text{cusp}}, \quad \gamma_0^{\text{cusp}} = 4, \quad \gamma_1^{\text{cusp}} = -\frac{80}{9}. \quad (51)$$

The regular anomalous dimension γ may be similarly expanded,

$$\gamma = \sum_{n=0}^{\infty} \left(\frac{\bar{\alpha}}{4\pi} \right)^{n+1} \gamma_n, \quad \gamma_0 = -6. \quad (52)$$

Using these expansions, the solution of Eq. (50) to any order is straightforward. Expressed in terms of the running coupling,

$$\begin{aligned} \log \left(\frac{H(\mu_L)}{H(\mu_H)} \right) &= -\frac{\gamma_0}{\beta_0} \left\{ \log r + \dots \right\} - \frac{\gamma_0^{\text{cusp}}}{\beta_0} \left\{ \log \frac{Q^2}{\mu_H^2} \log r + \frac{1}{\beta_0} \left[\frac{4\pi}{\alpha(\mu_H)} \left(\frac{1}{r} - 1 + \log r \right) \right. \right. \\ &\quad \left. \left. + \left(\frac{\gamma_1^{\text{cusp}}}{\gamma_0^{\text{cusp}}} - \frac{\beta_1}{\beta_0} \right) (-\log r + r - 1) - \frac{\beta_1}{2\beta_0} \log^2 r \right] + \dots \right\}, \end{aligned} \quad (53)$$

where $r = \alpha(\mu_L)/\alpha(\mu_H)$, and the first and second curly braces correspond to the terms $\gamma(\alpha)$ and $\gamma_{\text{cusp}}(\alpha)$ in Eq. (50), respectively.

We are interested in applications involving large logarithms such that $\alpha \log^2(\mu_H^2/\mu_L^2) \sim 1$. In this power counting, terms involving γ_0 scale as $\alpha^{1/2}$, and neglected terms involving $\gamma(\alpha)$ scale as $\alpha^{3/2}$. The leading terms involving the cusp anomalous dimension scale as α^0 , terms involving γ_1^{cusp} and β_1 scale as α^1 , and the remaining neglected terms scale as α^2 . When

¹¹ The term $16\pi^2(L-1)^2/3$ in $S^{(2)}$ has been noted in Ref. [39].

combined with one-loop matching computations, the terms retained in Eq. (53) are thus sufficient to ensure accuracy through order α^1 , accounting for logarithmic enhancements. The result (53) may be readily expressed in terms of the onshell coupling. Retaining terms through $\mathcal{O}(\alpha)$ in the above counting,

$$\begin{aligned} \log \left(\frac{H(\mu_L)}{H(\mu_H)} \right) &= \frac{\alpha}{4\pi} \left[-2 \log^2 \frac{\mu_H^2}{\mu_L^2} - 4 \log \frac{\mu_H^2}{\mu_L^2} \log \frac{Q^2}{\mu_H^2} + 6 \log \frac{\mu_H^2}{\mu_L^2} \right] \\ &+ \left(\frac{\alpha}{4\pi} \right)^2 \left[-\frac{8}{9} \log^3 \frac{\mu_H^2}{\mu_L^2} - \frac{8}{3} \log^2 \frac{\mu_H^2}{\mu_L^2} \left(\log \frac{Q^2}{\mu_H^2} - \log \frac{m^2}{\mu_L^2} \right) + \frac{76}{9} \log^2 \frac{\mu_H^2}{\mu_L^2} + \dots \right] \\ &+ \left(\frac{\alpha}{4\pi} \right)^3 \left[\frac{176}{27} \log^4 \frac{\mu_H^2}{\mu_L^2} + \dots \right] + \dots \end{aligned} \quad (54)$$

With the result (54), we have control over large logarithms and a complete solution through true order α (i.e., all neglected terms are parametrically small compared to order α , accounting for logarithmic enhancements). Setting $\mu_L \sim m$, inspection of $S(\mu_L)$ shows that the non-exponentiating term in $S^{(2)}$ is of order $\alpha^2 L^2 \sim \alpha^1$. $J(\mu_L)$ contains no large logarithms and may be truncated at one-loop order. $R(\mu_L)$ is nontrivial only at order $\alpha^{3/2}$, and may be neglected. Similarly, setting $\mu_H \sim M$, the matching coefficient $H(\mu_H)$ is free of large logarithms and may be truncated at one-loop order. Figure 5 compares successive inclusion of terms at order α^0 , $\alpha^{\frac{1}{2}}$ and α^1 in resummed perturbation theory. The figure demonstrates the necessity to control both leading and subleading logarithms in the perturbative expansion.

G. Nuclear recoil and structure corrections

The preceding discussion gives a complete solution including subleading log resummation for the idealized problem of scattering from a static source. Let us include the effects of nuclear recoil and structure. The “Born” cross section (denoted with subscript 0) is [6]

$$(d\sigma)_0 = (d\sigma)_{\text{Mott}} \frac{\epsilon G_E^2 + \tau G_M^2}{\epsilon(1 + \tau)}, \quad (55)$$

where the Mott cross section is now $(d\sigma/d\Omega)_{\text{Mott}} = \alpha^2 \cos^2(\theta/2)/[4\eta E^2 \sin^4(\theta/2)]$, with

$$\eta = E/E', \quad \tau = \frac{Q^2}{4M^2}, \quad \epsilon^{-1} = 1 + 2(1 + \tau) \tan^2 \frac{\theta}{2}, \quad (56)$$

and θ is the electron scattering angle in the lab frame. To begin, we work to first order in nuclear charge, i.e., neglect radiative corrections involving the proton. The experimentally

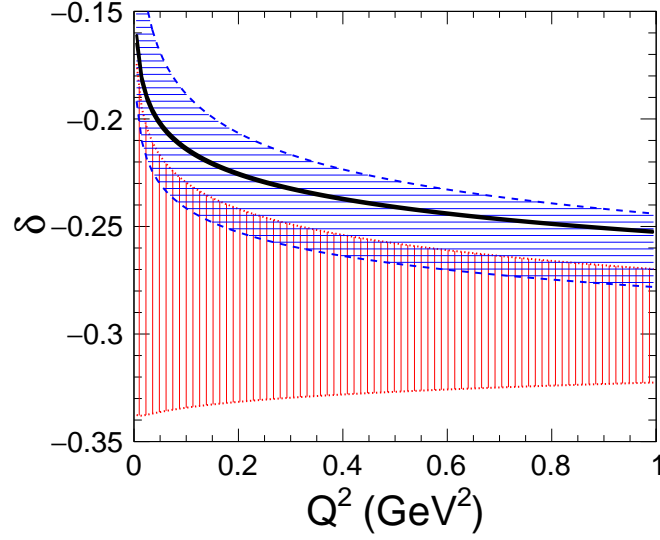


FIG. 5: Radiative correction factor δ from Eq. (26) in resummed perturbation theory for the static source limit of electron-proton scattering, with $E = 1 \text{ GeV}$, $\Delta E = 5 \text{ MeV}$. The bands represent the impact of varying $\min(Q^2, E^2)/2 < \mu_H^2 < 2 \max(Q^2, E^2)$ and $\min(m^2, \Delta E^2)/2 < \mu_L^2 < 2 \max(m^2, \Delta E^2)$, using leading log resummation (blue, horizontal stripes) next-to-leading log resummation (red, vertical stripes) and complete next-to-leading order resummation (black, solid band).

measured cross section is

$$d\sigma = \frac{(d\sigma)_0}{[1 - \hat{\Pi}(q^2)]^2} (1 + \delta_e + \delta_{e\gamma} + \delta_{e\gamma\gamma} + \dots) \equiv \frac{(d\sigma)_0}{[1 - \hat{\Pi}(q^2)]^2} (1 + \delta). \quad (57)$$

The virtual corrections as a function of q^2 are identical to the static case,

$$\delta_e = |F_q(q^2, m^2, \lambda^2)|^2 - 1. \quad (58)$$

First order real corrections are now [40]

$$\delta_{e\gamma}^{(1)} = 4 \left(\log \frac{(\eta \Delta E)^2}{EE'} - \log \frac{\lambda^2}{m^2} \right) (L - 1) + 2L^2 - 2 \log^2 \eta + 4 \text{Li}_2 \left(1 - \frac{Q^2 \eta}{4E^2} \right) - \frac{4\pi^2}{3}. \quad (59)$$

In terms of this result, second order real corrections are

$$\delta_{e\gamma\gamma}^{(2)} = \frac{1}{2!} [\delta_{e\gamma}^{(1)}]^2 - \frac{16\pi^2}{3} (L - 1)^2. \quad (60)$$

Assuming soft-collinear factorization (cf. the discussion around Eq. (31) and Appendix D), the mixed real-virtual contribution at second order is given in terms of the result (59) by

$$\delta_{e\gamma}^{(2)} = \delta_e^{(1)} \delta_{e\gamma}^{(1)}. \quad (61)$$

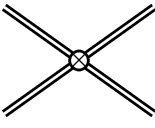
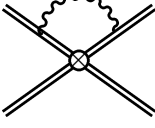
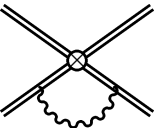
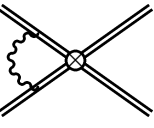
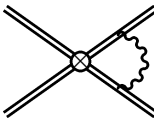
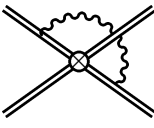
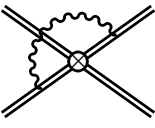
The results (58), (59), (60) and (61) imply that Eq.(32) remains valid when recoil effects are included. These results are valid at first order in nuclear charge, and in the regime $m \ll E$, but with the restriction $E \ll M$ removed.

H. Two photon exchange

The complete result at first order in nuclear charge is simplified by the factorization theorem which implies that recoil effects are confined to soft function contributions involving real emission. Beyond first order in the nuclear charge, radiative corrections introduce new operators at the hard scale, and sensitivity to nuclear structure beyond form factors. Let us briefly discuss the inclusion of such corrections in the formalism.

The factorization formula including second (and higher) order corrections in nuclear charge takes the same form as Eq. (33). The function $J(\mu)$ is unchanged. The function $R(\mu)$ may be taken as unity at the relevant order [recall $R \sim \alpha^2 L = \mathcal{O}(\alpha^{3/2})$, in our counting $\alpha L^2 = \mathcal{O}(1)$]. Let us focus on the hard and soft functions. In particular, let us consider the extraction of proton structure information from scattering data. Our goal is to isolate $H(\mu = M)$, which is built from conventionally defined Born form factors, as in Eq. (12), and analogous hard coefficient functions arising from two-photon exchange. In the absence of sufficient data [41] to simultaneously extract the Born form factors and the two-photon exchange contributions to $H(\mu = M)$, hadronic models are employed for the latter [42, 43].

The soft function (as well as the remainder function R and jet function J) is universal to all of the underlying amplitudes. In place of the static-source limit of Eq. (9), we have now

$$\begin{aligned}
\sqrt{S(\mu, \Delta E = 0)} &= Z_h^{(e)} Z_h^{(p)} \left| \begin{array}{cccc}

+

+

+

\end{array} \right. \\
&+ \left| \begin{array}{ccc}

+

+

\end{array} \right| \\
&= 1 - \frac{\alpha}{2\pi} \text{Re} \left\{ [u \cdot u' f(u \cdot u') - 1] + Z^2 [v \cdot v' f(v \cdot v') - 1] \right. \\
&\quad + Z [u \cdot v f(-u \cdot v - i0) + u' \cdot v' f(-u' \cdot v' - i0) + u \cdot v' f(u \cdot v') \\
&\quad \left. + u' \cdot v f(u' \cdot v)] \right\} \log \frac{\mu^2}{\lambda^2}, \tag{62}
\end{aligned}$$

where u^μ , u'^μ are timelike vectors proportional to initial and final electron momentum, and v^μ , v'^μ similarly correspond to the momenta of the initial and final state proton. The function $f(w)$ was introduced for $w \geq 1$ in Eq. (6), and the explicit evaluation of the Feynman integrals yields

$$f(-w - i0) = -f(w) + \frac{i\pi}{\sqrt{w^2 - 1}}. \quad (63)$$

The kinematic constraints,

$$v' \cdot u = v \cdot u', \quad v' \cdot u' = v \cdot u, \quad (64)$$

may be used to reduce the number of terms appearing in Eq. (62). Real radiation contributions to the soft function are computed using the integrals of Appendix C. After simplification, the complete soft function reads

$$\begin{aligned} S = 1 + \frac{\alpha}{4\pi} & \left\{ 4 \left(\log \frac{(\eta \Delta E)^2}{EE'} - \log \frac{\mu^2}{m^2} \right) (L - 1) + 2L^2 - 2 \log^2 \eta + 4 \text{Li}_2 \left(1 - \frac{Q^2 \eta}{4E^2} \right) - \frac{4\pi^2}{3} \right. \\ & + 8Z \left[\log \eta \log \frac{4\eta^2}{w_+} + \text{Li}_2 \left(1 - \frac{\eta}{w_+} \right) - \text{Li}_2 \left(1 - \frac{1}{\eta w_+} \right) + \log \eta \log \frac{\mu^2}{(\Delta E)^2} \right] \\ & \left. + 4Z^2 \left[(wf(w) - 1) \log \frac{4\eta^2 (\Delta E)^2}{\mu^2} + 1 - \frac{w}{\sqrt{w^2 - 1}} \left\{ \log^2 w_+ - \log w_+ + \text{Li}_2 \left(1 - \frac{1}{w_+^2} \right) \right\} \right] \right\}. \end{aligned} \quad (65)$$

In order to extract the hard function at scale $\mu = M$, we write the process as

$$d\sigma \propto H(M) \times \frac{H(\mu)}{H(M)} \times (JRS)(\mu) \equiv H(M)(1 + \delta), \quad (66)$$

where δ is the total radiative correction. Evaluating J , R and S at the soft scale, we thus require the ratio $H(\mu)/H(M)$, with control over large logarithms in perturbation theory.

The renormalization of the hard function is now governed by (cf. Appendix A)

$$\frac{d \log H}{d \log \mu} = 2 \left[\gamma_{\text{cusp}}(\bar{\alpha}) \log \frac{Q^2}{\mu^2} + \gamma_{\text{cusp}}(v \cdot v', \bar{\alpha}) + 2\gamma_{\text{cusp}}(\bar{\alpha}) \log \frac{v \cdot p'}{-v \cdot p - i0} + \gamma(\bar{\alpha}) \right]. \quad (67)$$

The cusp function $\gamma_{\text{cusp}}(\bar{\alpha})$ has been introduced above in Eq. (50), $\gamma_{\text{cusp}}(w, \bar{\alpha})$ is given in Eq. (A7), and the regular anomalous dimension $\gamma(\bar{\alpha})$ is

$$\gamma = \sum_{n=0}^{\infty} \left(\frac{\bar{\alpha}}{4\pi} \right)^{n+1} \gamma_n, \quad \gamma_0 = -10. \quad (68)$$

The solution to Eq. (67), analogous to Eq. (53), is

$$\log \frac{H(\mu_L)}{H(\mu_H)} = -\frac{1}{\beta_0} \left[\gamma_0 + \left(\log \frac{Q^2}{\mu_H^2} + wf(w) + 2 \log \frac{E'}{-E - i0} \right) \gamma_0^{\text{cusp}} \right] \log r$$

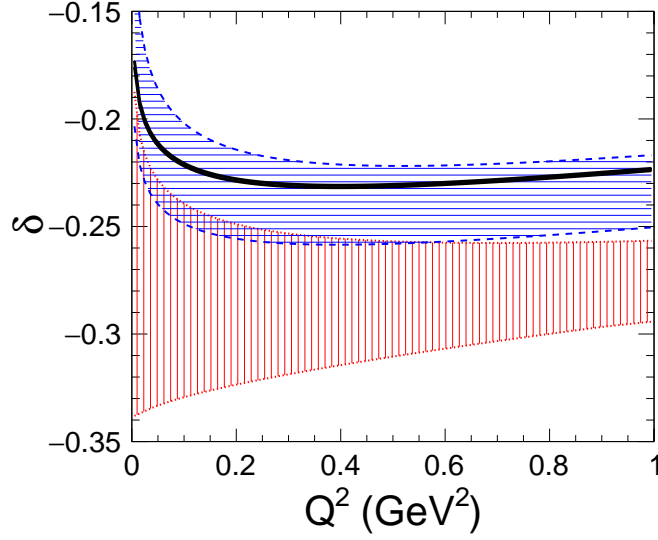


FIG. 6: Same as Fig. 5, but including recoil and nuclear charge corrections (i.e., two photon exchange and proton vertex corrections). The total radiative correction δ is given by Eq. (66).

$$-\frac{\gamma_0^{\text{cusp}}}{\beta_0^2} \left\{ \frac{4\pi}{\alpha(\mu_H)} \left(\frac{1}{r} - 1 + \log r \right) + \left(\frac{\gamma_1^{\text{cusp}}}{\gamma_0^{\text{cusp}}} - \frac{\beta_1}{\beta_0} \right) (-\log r + r - 1) - \frac{\beta_1}{2\beta_0} \log^2 r + \dots \right\}. \quad (69)$$

Expressed in terms of onshell coupling,

$$\begin{aligned} \log \frac{H(\mu_L)}{H(\mu_H)} = & \left\{ \frac{\alpha}{4\pi} \left[-2 \log^2 \frac{\mu_H^2}{\mu_L^2} - 4 \log \frac{\mu_H^2}{\mu_L^2} \log \frac{Q^2}{\mu_H^2} \right] \right. \\ & + \left(\frac{\alpha}{4\pi} \right)^2 \left[-\frac{8}{9} \log^3 \frac{\mu_H^2}{\mu_L^2} - \frac{8}{3} \log^2 \frac{\mu_H^2}{\mu_L^2} \left(\log \frac{Q^2}{\mu_H^2} - \log \frac{m^2}{\mu_L^2} \right) + \frac{40}{9} \log^2 \frac{\mu_H^2}{\mu_L^2} + \dots \right] \\ & + \left(\frac{\alpha}{4\pi} \right)^3 \left[\frac{176}{27} \log^4 \frac{\mu_H^2}{\mu_L^2} + \dots \right] + \dots \Big\} + \left[-10 + 4wf(w) + 8 \log \frac{E'}{-E - i0} \right] \\ & \times \left\{ \frac{\alpha}{4\pi} \left[-\log \frac{\mu_H^2}{\mu_L^2} \right] + \left(\frac{\alpha}{4\pi} \right)^2 \left[-\frac{2}{3} \log^2 \frac{\mu_H^2}{\mu_L^2} + \dots \right] + \dots \right\}. \quad (70) \end{aligned}$$

where terms through α^1 are retained, in the counting $\alpha \log^2(Q^2/m^2) \sim 1$. The impact of successive terms in the resummed perturbative expansion is displayed in Fig. 6.

IV. DISCUSSION

The precision of electron-proton scattering experiments has reached a level demanding systematic analysis of subleading radiative corrections at two loop order and beyond. We

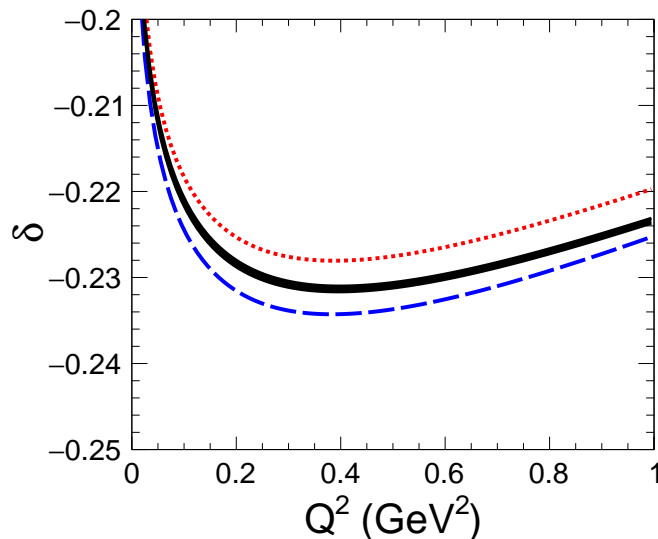


FIG. 7: Comparison of complete next to leading order resummed correction (solid black band) to naive exponentiations using different factorization scales for the two photon exchange correction: $\mu^2 = M^2$ (dotted red line) and $\mu^2 = Q^2$ (dashed blue line). See text for details.

have presented the general framework that separates physical scales in the scattering process, allowing a systematic merger of fixed order perturbation theory with large log resummation.

The quantum field theory analysis reveals implicit conventions and assumptions that often differ between applications, such as between scattering and bound state problems. The definition of the proton charge and magnetic radii in the presence of electromagnetic radiative corrections is naturally defined in Eq. (12). A comparison to other definitions in the literature is presented in Appendix B. The separation of soft and hard scales in two photon exchange is similarly ambiguous in standard treatments. The common Maximon-Tjon convention [40] implicitly takes momentum-dependent factorization scale $\mu^2 = Q^2$ for two-photon exchange, in conflict with the Q^2 -independent choice $\mu^2 = M^2$ that is closest to the implicit convention for vertex corrections.

The exponentiation and cancellation of infrared singularities [10] in physical processes has often been used to motivate a simple exponentiation of first order corrections in order to resum logarithmically enhanced radiative corrections at second- and higher-order in perturbation theory [7, 44]. This procedure fails to capture subleading logarithms, beginning

at order $\alpha^2 L^3 = \mathcal{O}(\alpha^{\frac{1}{2}})$, in our counting $\alpha L^2 = \mathcal{O}(1)$, cf. Eq. (32). These large logarithms are automatically generated in the renormalization analysis that the effective theory makes possible. The convergence of resummed perturbation theory is illustrated, for the complete problem including proton structure and recoil, in Fig. 6. A comparison of the resummed prediction to the naive exponentiation ansatz is displayed in Fig. 7.

Also shown in Fig. 7 is the variation due to different scale choices implicit in different two-photon exchange corrections.¹² These ansatzes differ at the percent level in the considered kinematic range, and fall well outside the error band represented by the complete next-to-leading order resummed prediction.

Special attention has been paid to the effects of real emission beyond tree level. Soft-photon factorization and exponentiation is readily proven [10] for the case $\Delta E \ll m$. In practical experiments, the opposite limit, $m \ll \Delta E$, obtains. It is readily seen (cf. Appendix D) that multiple low-energy momentum regions appear, invalidating a simple factorization argument. Nevertheless, an explicit computation of the two-loop mixed real-virtual correction demonstrates factorization for the simplest elastic scattering observable under consideration. Extensions to other observables, including the possibility of hard photon emission, will be considered elsewhere.

Discrepancies at the 0.5 – 1% level exist between the complete resummed prediction (70), and phenomenological approximations employed in the analysis of A1 collaboration electron-proton scattering data [7], as illustrated in Fig. 7. It is interesting to consider the impact of these corrections on the proton radius puzzle. These discrepancies are in tension with the 0.2 – 0.5% systematic errors assumed in the extraction of proton electric and magnetic charge radii [7], but will be partially absorbed by floating normalization parameters in fits to independent datasets [6, 7]. A careful accounting of correlated shape variations induced by radiative corrections must also be accounted for when fitting the inferred radiative tail for the signal process together with background processes [7, 46]. The complete implementation of improved corrections in the analysis of electron-proton scattering data, for charge radius and form factor extractions, is outside the scope of this paper [47]. It is straightforward

¹² For example, the so-called McKinley-Feshbach correction [45] represents the large- M limit of the hard-coefficient contribution to two-photon exchange, and is independent of factorization scale μ . Using this correction [7] results in an irreducible factorization-scale uncertainty, uncanceled between matrix element and coefficient.

to include these improvements in event generators [44, 48–50]. It is interesting to perform a systematic analysis of power corrections, particularly of relevance to very low Q^2 and/or high ΔE [51, 52].¹³

Many other lepton-hadron processes are being probed at the percent and permille level, and are critical to next generation experiments probing fundamental physics in and beyond the standard model. Examples include neutrino-nucleus scattering for neutrino oscillations [53], $e^+e^- \rightarrow$ hadrons for input to $(g-2)_\mu$ [54], and parity violating scattering observables [55–57]. The effective field theory analysis may be readily applied to systematically compute radiative corrections involving large logarithms in these and other applications.

Acknowledgments. The author thanks J. Arrington and G. Lee for collaboration on Ref. [6] which motivated the present work, and T. Becher, G. Paz and J. Sapirstein for comments on the manuscript. Research supported by a NIST Precision Measurement Grant and the U.S. Department of Energy, Office of Science, Office of High Energy Physics (DOE Grant No. DE-FG02-13ER41958). TRIUMF receives federal funding via a contribution agreement with the National Research Council of Canada. Research at Perimeter Institute is supported by the Government of Canada through the Department of Innovation, Science and Economic Development and by the Province of Ontario through the Ministry of Research and Innovation.

Appendix A: Renormalization constants

We collect here standard renormalization constants and conventions used in the paper. Working in $d = 4 - 2\epsilon$ dimensions, the bare QED coupling e_{bare} and fine structure constant α_{bare} are defined and related to the $\overline{\text{MS}}$ fine structure constant $\bar{\alpha} \equiv \alpha(\mu)$ by

$$\frac{e_{\text{bare}}^2}{4\pi} (4\pi)^\epsilon e^{-\gamma_E \epsilon} = \alpha_{\text{bare}} = \mu^{2\epsilon} \bar{\alpha} \left[1 + \sum_{n=0}^{\infty} Z_n \left(\frac{\bar{\alpha}}{4\pi} \right)^{n+1} \right], \quad Z_0 = \frac{4}{3\epsilon}. \quad (\text{A1})$$

The QED beta function is defined as

$$\frac{d\bar{\alpha}}{d \log \mu} = -2\bar{\alpha} \sum_{n=0}^{\infty} \beta_n \left(\frac{\bar{\alpha}}{4\pi} \right)^{n+1}, \quad \beta_0 = -\frac{4}{3}n_f, \quad \beta_1 = -4n_f. \quad (\text{A2})$$

¹³ First order power corrections in the static source limit are obtained from the integrals in Sec. C. These are small in the kinematics of the A1 collaboration data [7].

The relation between onshell and $\overline{\text{MS}}$ couplings with $n_f = 1$ light flavors of mass m is (in $d = 4$)

$$\bar{\alpha} \equiv \alpha(\mu) = \alpha \left[1 + \sum_{n=0}^{\infty} z_n \left(\frac{\alpha}{4\pi} \right)^{n+1} \right], \quad z_0 = \frac{8}{3} \log \frac{\mu}{m}, \quad z_1 = \frac{64}{9} \log^2 \frac{\mu}{m} + 8 \log \frac{\mu}{m} + 15. \quad (\text{A3})$$

The onshell wavefunction renormalization constants for massive relativistic (QED) and non-relativistic (NRQED) fermions are

$$Z_\Psi = 1 + \frac{\bar{\alpha}}{4\pi} \left(-\frac{1}{\epsilon} + \log \frac{m^2}{\mu^2} - 2 \log \frac{\lambda^2}{m^2} - 4 \right), \quad Z_h = 1 + \frac{\bar{\alpha}}{4\pi} \left(\frac{2}{\epsilon} - 2 \log \frac{\lambda^2}{\mu^2} \right). \quad (\text{A4})$$

Consider the renormalization of Wilson coefficients for operators representing the soft and collinear matrix elements for physical amplitudes specified by external momenta of a given collection of massless and massive fermions. Let the massless (ψ) and massive (h) fermions be labeled by lowercase indices i , and uppercase indices I , respectively. In general, [58–61]

$$\begin{aligned} \frac{d \log C}{d \log \mu} = & \sum_{\{i,j\}} Q_i Q_j \gamma_{\text{cusp}}(\bar{\alpha}) \log \frac{\mu^2}{-s_{ij}} - \sum_{\{I,J\}} Q_I Q_J \gamma_{\text{cusp}} \left(\frac{-s_{IJ}}{M_I M_J}, \bar{\alpha} \right) \\ & + \sum_{\{I,j\}} Q_I Q_j \gamma_{\text{cusp}}(\bar{\alpha}) \log \frac{M_I \mu}{-s_{Ij}} + \sum_i \gamma^h(\bar{\alpha}) + \sum_I \gamma^\psi(\bar{\alpha}), \end{aligned} \quad (\text{A5})$$

where sums $\{i, j\}$ run over sets of distinct particle indices. Here Q_i denotes the electric charge (in units of the proton charge) of the fermion, with all lines in a Feynman diagram viewed as ingoing (so, e.g., $Q_i = -1$ for an incoming electron, $Q_i = +1$ for an outgoing electron). Also, $s_{ij} = 2p_i \cdot p_j + i0$, where all momenta are viewed as incoming.

Here the massless cusp function is

$$\gamma_{\text{cusp}}(\bar{\alpha}) = \sum_{n=0}^{\infty} \left(\frac{\bar{\alpha}}{4\pi} \right)^{n+1} \gamma_n^{\text{cusp}}, \quad \gamma_0^{\text{cusp}} = 4, \quad \gamma_1^{\text{cusp}} = -\frac{80}{9} n_f. \quad (\text{A6})$$

The massive cusp function is

$$\gamma_{\text{cusp}}(w, \bar{\alpha}) = \gamma_{\text{cusp}}(\bar{\alpha}) w f(w), \quad (\text{A7})$$

with $f(w)$ as in Eq. (6) and $\gamma_{\text{cusp}}(\bar{\alpha})$ as in Eq. (A6). The one-particle terms for massless fermions are

$$\gamma^\psi = \sum_{n=0}^{\infty} \left(\frac{\bar{\alpha}}{4\pi} \right)^{n+1} \gamma_n^\psi, \quad \gamma_0^\psi = -3, \quad (\text{A8})$$

while for massive fermions

$$\gamma^h = \sum_{n=0}^{\infty} \left(\frac{\bar{\alpha}}{4\pi} \right)^{n+1} \gamma_n^h, \quad \gamma_0^h = -2, \quad \gamma_1^h = \frac{40}{9} n_f. \quad (\text{A9})$$

With these general results, we obtain the anomalous dimensions for hard functions in Eqs. (21), (50) and (67). In particular, in Eq. (21) we identify $\Gamma_{\text{cusp}}(w, \bar{\alpha}) = \gamma_{\text{cusp}}(w, \bar{\alpha}) + 2\gamma^h(\bar{\alpha})$. In Eq. (50) we identify $\gamma = 2\gamma^\psi$, and in Eq. (67) we identify $\gamma = 2\gamma^\psi + 2\gamma^h$.

Appendix B: Born conventions

A number of conflicting conventions exist in the electron-proton scattering literature for defining infrared finite Born form factors. These must all be of the form,

$$F_i(q^2)^{\text{Born}} \equiv \tilde{F}_i(q^2) \left\{ 1 - \frac{Z^2 \alpha}{2\pi} \left[(wf(w) - 1) \log \frac{M^2}{\lambda^2} + \Delta K \right] + \mathcal{O}(\alpha^2) \right\}, \quad (\text{B1})$$

as derived in the effective theory analysis. Here \tilde{F}_i denotes the onshell form factor, and $F_i^{\text{Born}}(0) = \tilde{F}_i(0)$. Several conventions are listed here for the finite term ΔK . The natural convention based on the factorization formulas discussed in this paper is

$$\Delta K^{\text{fac.}} = 0. \quad (\text{B2})$$

The convention adopted in Ref. [6] is essentially that of Maximon and Tjon [40], but neglecting an additional model-dependent correction (referred to as $\delta_{\text{el}}^{(1)}$ in Ref. [40]),

$$\begin{aligned} \Delta K^{\text{LAH}} &= \frac{w}{\sqrt{w^2 - 1}} \left[\log w_+ \log[2(w + 1)] - 2\text{Li}_2 \left(\frac{-1}{w_+} \right) - \frac{\pi^2}{6} - \frac{1}{2} \log^2 w_+ \right] \\ &= -\frac{q^2}{6M^2} + \mathcal{O}(Q^4), \end{aligned} \quad (\text{B3})$$

where in the last line, the result is expanded around $Q^2 = 2M^2(w - 1) \rightarrow 0$.

There are also several conventions in the atomic physics literature for ΔK , or equivalently for the proton electron and magnetic radii. Let us define

$$\begin{aligned} \frac{1}{6} r_E^2 &\equiv \frac{1}{G_E(0)} \left. \frac{dG_E^{\text{Born}}}{dq^2} \right|_{q^2=0} \\ &= \tilde{F}_1'(0) + \frac{F_2(0)}{4M^2} - \frac{Z^2 \alpha}{2\pi M^2} \left[\frac{2}{3} \log \frac{M^2}{\lambda^2} - M^2 \Delta K'(0) \right]. \end{aligned} \quad (\text{B4})$$

The case $\Delta K'(0) = 0$, as for ΔK^{fac} in Eq. (B2), corresponds to the convention used in Ref. [62]; in this convention, the charge radius of a point particle vanishes including $\mathcal{O}(\alpha)$ radiative corrections. With the convention (B3), we have instead

$$(r_E^2)^{\text{LAH}} = (r_E^2)^{\text{fac.}} - \frac{Z^2 \alpha}{2\pi M^2}. \quad (\text{B5})$$

Several other conventions have been used, e.g. Pachucki's definition in Ref. [63] implies

$$(r_E^2)^{\text{P}} = (r_E^2)^{\text{fac.}} - \frac{5Z^2 \alpha}{3\pi M^2}. \quad (\text{B6})$$

Formula (B4) may be used to translate the radius used in other conventions.

Appendix C: Phase space integrals

We list here expressions for phase space integrals used in the paper. In terms of arbitrary timelike unit vectors v^μ and v'^μ , [64]

$$\begin{aligned} \int_{\ell^0 \leq \Delta E} \frac{d^3 \ell}{(2\pi)^3 2\ell^0} \frac{1}{(v \cdot \ell)(v' \cdot \ell)} &= \frac{1}{8\pi^2 \sqrt{w^2 - 1}} \left[2 \log(w_+) \log \frac{2\Delta E}{\lambda} + \log^2(v_+^0) - \log^2(v_+'^0) \right. \\ &+ \text{Li}_2 \left(1 - \frac{v_+^0}{\sqrt{w^2 - 1}} (w_+ v^0 - v'^0) \right) + \text{Li}_2 \left(1 - \frac{v_-^0}{\sqrt{w^2 - 1}} (w_+ v^0 - v'^0) \right) \\ &\left. - \text{Li}_2 \left(1 - \frac{v_+^0}{\sqrt{w^2 - 1}} (v^0 - w_- v'^0) \right) - \text{Li}_2 \left(1 - \frac{v_-^0}{\sqrt{w^2 - 1}} (v^0 - w_- v'^0) \right) \right]. \end{aligned} \quad (\text{C1})$$

In the limit $v' = v$, Eq. (C1) becomes

$$\int_{\ell^0 \leq \Delta E} \frac{d^3 \ell}{(2\pi)^3 2\ell^0} \frac{1}{(v \cdot \ell)^2} = \frac{1}{4\pi^2} \left[\log \frac{2\Delta E}{\lambda} - \frac{v^0}{\sqrt{(v^0)^2 - 1}} \log(v^0 + \sqrt{(v^0)^2 - 1}) \right]. \quad (\text{C2})$$

In the analysis of power corrections (in $\Delta E/E$), we encounter integrals with the replacement $p' \rightarrow \tilde{p}'^\mu$, where \tilde{p}'^μ is defined with energy $\tilde{E}' = E' - \ell^0$ (recall $E' = E$ for the static limit) and spatial momentum in the direction identical to p'^μ . The first class of integrals is unchanged,

$$\int_{\ell^0 \leq \Delta E} \frac{d^3 \ell}{(2\pi)^3 2\ell^0} \frac{m^2}{(\tilde{p}' \cdot \ell)^2} = \int_{\ell^0 \leq \Delta E} \frac{d^3 \ell}{(2\pi)^3 2\ell^0} \frac{m^2}{(p' \cdot \ell)^2} \rightarrow \frac{1}{4\pi^2} \left[\log \frac{\Delta E}{E} - \log \frac{\lambda}{m} \right], \quad (\text{C3})$$

where the arrow indicates the large energy limit, $v^0 = E/m \rightarrow \infty$. For the second class of integrals,

$$\begin{aligned} \int_{\ell^0 \leq \Delta E} \frac{d^3 \ell}{(2\pi)^3 2\ell^0} \frac{2p \cdot \tilde{p}'}{(p \cdot \ell)(\tilde{p}' \cdot \ell)} &\rightarrow \frac{1}{8\pi^2} \left[4 \left(\log \frac{\Delta E}{E} + \log \frac{\lambda}{m} \right) L + L^2 + 2\text{Li}_2 \left(\cos^2 \frac{\theta}{2} \right) - \frac{2\pi^2}{3} \right. \\ &\left. \frac{\Delta E}{E} (-8L + 4) + \dots \right], \end{aligned} \quad (\text{C4})$$

where the first order power correction is displayed.

Appendix D: Two loop mixed real-virtual correction: full theory

Here we give details on the explicit evaluation of the two-loop matching calculation for electron-proton scattering involving mixed real-virtual corrections in the static source limit. Recall the tree level squared matrix element for the process without photon emission,

$$\sum |\mathcal{M}_0|^2 = e^2 \text{Tr}[(\not{p}' + m)\gamma^0(\not{p} + m)\gamma^0]. \quad (\text{D1})$$

The squared matrix element for the process with photon emission is

$$\sum |\mathcal{M}_{1,\text{tree}}|^2 = \sum |\mathcal{M}_0|^2 e^2 \left[\frac{2p \cdot p'}{p \cdot \ell p' \cdot \ell} - \frac{m^2}{(p \cdot \ell)^2} - \frac{m^2}{(p' \cdot \ell)^2} \right], \quad (\text{D2})$$

where terms yielding power suppressed contributions after photon phase space integration have been dropped.

In the analysis of the phase space integrals for loop corrections to Eq. (D2), we encounter integrals of the form

$$I_1 = \int \frac{d^3\ell}{\ell^0} \frac{m^2}{(p \cdot \ell)^2} f(a), \quad I_2 = \int \frac{d^3\ell}{\ell^0} \frac{m^2}{(p' \cdot \ell)^2} g(b), \quad I_3 = \int \frac{d^3\ell}{\ell^0} \frac{2p \cdot p'}{p \cdot \ell p' \cdot \ell} h(a, b), \quad (\text{D3})$$

where we introduce the shorthand $a = -p' \cdot \ell/m^2 - i0$, $b = p \cdot \ell/m^2$. Introduce the small parameter $\kappa = m/E$. For simplicity in this description, consider the case of backward scattering where $\mathbf{p}' = -\mathbf{p}$. Introduce a light-cone basis for the photon momentum,

$$\ell^\mu = (n \cdot \ell \bar{n} \cdot \ell, \ell_\perp^\mu), \quad (\text{D4})$$

where n and \bar{n} are lightlike vectors in the direction of p and p' , with $n^2 = \bar{n}^2 = 0$, $n \cdot \bar{n} = 2$. For I_1 , the leading contribution is readily found to arise from momenta scaling as

$$k^\mu \sim E(\kappa, \kappa^3, \kappa^2) : \quad I_1 \sim f(\kappa) \rightarrow f(0), \quad (\text{D5})$$

i.e., from photons that are both soft and collinear to the final state electron. Contributions from other regions involve power suppression, e.g.

$$\begin{aligned} k^\mu \sim E(\kappa, \kappa, \kappa) : \quad I_1 &\sim \kappa^2 f(\kappa^{-1}), \\ k^\mu \sim E(\kappa^2, \kappa^2, \kappa^2) : \quad I_1 &\sim \kappa^2 f(\kappa^0). \end{aligned} \quad (\text{D6})$$

Similarly, for I_2 , the leading contribution is from photons that are both soft and collinear to the initial state electron,

$$k^\mu \sim E(\kappa^3, \kappa, \kappa^2) : \quad I_2 \sim g(\kappa) \rightarrow g(0). \quad (\text{D7})$$

Finally, for I_3 , multiple regions potentially contribute.

$$\begin{aligned}
k^\mu &\sim E(\kappa, \kappa, \kappa) : & I_3 &\sim h(\kappa^{-1}, \kappa^{-1}), \\
k^\mu &\sim E(\kappa^3, \kappa, \kappa^2) : & I_3 &\sim h(\kappa, \kappa^{-1}), \\
k^\mu &\sim E(\kappa, \kappa^3, \kappa^2) : & I_3 &\sim h(\kappa^{-1}, \kappa), \\
k^\mu &\sim E(\kappa^2, \kappa^2, \kappa^2) : & I_3 &\sim h(\kappa^0, \kappa^0).
\end{aligned} \tag{D8}$$

Inside loops, the presence of multiple momentum modes of the same virtuality ($L^2 \sim \kappa^4$) complicates a simple argument for soft-collinear factorization based on eikonal decoupling (cf. the discussion surrounding Eq. (8), where only a single, soft, momentum mode is present).¹⁴ We proceed by direct evaluation of the diagrams.

The relevant squared matrix element contains interference terms between the tree-level real radiation diagrams of Fig. 1 and the one loop real radiation diagrams of Fig. 2. After averaging and summing over initial and final electron spins, the squared matrix element, divided by the tree level squared matrix element without radiation, can be expanded in terms of the following basic integrals (and the integrals related by $p \leftrightarrow p'$, $\ell \leftrightarrow -\ell$),

$$\begin{aligned}
&\int \frac{1}{D_1(\lambda)D_2D_3D_4}, \quad \int \frac{1}{D_1D_2D_3D_4} [1, L^\mu, L^\mu L^\nu, L^\mu L^\nu L^\rho], \quad \int \frac{1}{D_1D_2D_4} [1, L^\mu, L^\mu L^\nu], \\
&\int \frac{1}{D_1D_3D_4} [1, L^\mu, L^\mu L^\nu], \quad \int \frac{1}{D_1D_4} [1, L^\mu], \tag{D9}
\end{aligned}$$

where integration is over $\int = \int d^d L$, and the denominators are

$$\begin{aligned}
D_1(\lambda) &= L^2 - \lambda^2, \quad D_1 = L^2, \quad D_2 = L^2 + 2L \cdot p, \quad D_3 = L^2 + 2L \cdot p', \\
D_4 &= L^2 + 2L \cdot (p' + \ell) + 2p' \cdot \ell. \tag{D10}
\end{aligned}$$

We evaluated these integrals using dimensional regularization for ultraviolet divergences and photon mass λ for infrared divergences. After mass, coupling and wavefunction renormalization, and expressing the result in terms of the onshell coupling, we obtain expressions of the form (D3), which may be expanded according to Eqs. (D5), (D7) and (D8). Neglecting contributions that are power suppressed after photon phase space integration, the final result reads

$$\sum |\mathcal{M}_1|^2 = \sum |\mathcal{M}_0|^2 e^2 \left[\frac{2p \cdot p'}{p \cdot \ell p' \cdot \ell} - \frac{m^2}{(p \cdot \ell)^2} - \frac{m^2}{(p' \cdot \ell)^2} \right] \left\{ 1 + \frac{\alpha}{4\pi} \left[-2 \log^2 \frac{Q^2}{m^2} \right. \right.$$

¹⁴ For a related discussion on potential difficulties with naive factorization, see Ref. [34].

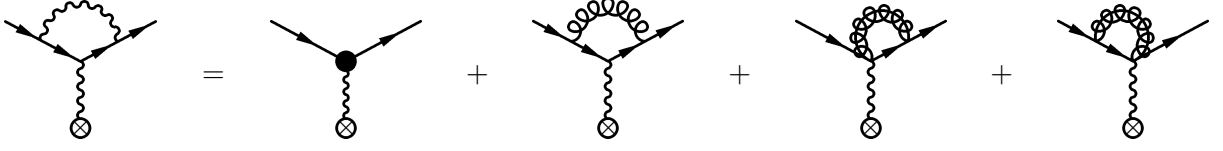


FIG. 8: Expansion in momentum regions of amplitudes for electron scattering in the static source limit. Diagram on the left hand side is in the full theory (QED), diagrams on the right hand side are in the effective theory. Soft and collinear photons are represented by curly lines, and curly lines superimposed on solid lines, respectively.

$$+ 8 \log \frac{\lambda}{m} \left(\log \frac{Q^2}{m^2} - 1 \right) + 6 \log \frac{Q^2}{m^2} + \frac{2\pi^2}{3} - 8 \Big] \Big\}. \quad (\text{D11})$$

Appendix E: Two loop mixed real-virtual correction: effective theory

Here we outline the evaluation of the mixed real-virtual corrections using a decomposition into soft and collinear momentum regions, formalized as soft-collinear effective theory [18–25]. We first review the analysis of vertex corrections.

1. Vertex corrections

Consider the amplitude pictured on the left hand side of Fig. 8,

$$\delta F \gamma^\mu = -ie^2 \int \frac{d^d L}{(2\pi)^d} \gamma^\alpha (\not{L} + \not{p}' + m) \gamma^\mu (\not{L} + \not{p} + m) \gamma_\alpha \frac{1}{L^2 - \lambda^2} \frac{1}{L^2 + 2L \cdot p} \frac{1}{L^2 + 2L \cdot p'}, \quad (\text{E1})$$

and the corresponding decomposition pictured on the right hand side of Fig. 8. Introduce light-cone vectors n^μ and \bar{n}^μ for the direction p^μ , and corresponding vectors n'^μ and \bar{n}'^μ for the direction p'^μ . The hard contribution is represented by the first diagram on the right hand side of Fig. 8, and is obtained from

$$\begin{aligned} \delta F_H \gamma^\mu &= -ie^2 \int \frac{d^d L}{(2\pi)^d} \gamma^\alpha (\not{L} + \not{p}'_-) \gamma^\mu (\not{L} + \not{p}_-) \gamma_\alpha \frac{1}{L^2} \frac{1}{L^2 + 2L \cdot p_-} \frac{1}{L^2 + 2L \cdot p'_-}, \\ &= -ie^2 \gamma^\mu [c_\epsilon] Q^{-2\epsilon} \left[-\frac{2}{\epsilon^2} - \frac{3}{\epsilon} - 8 + \frac{\pi^2}{3} \right], \end{aligned} \quad (\text{E2})$$

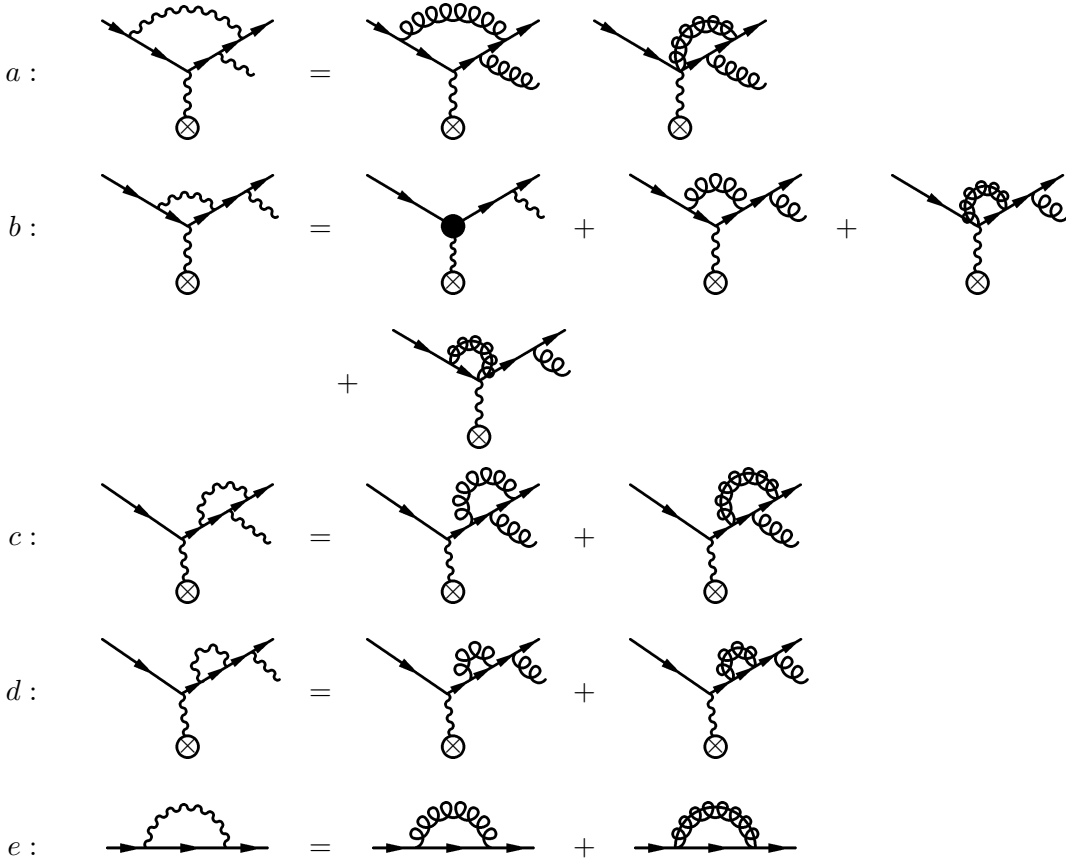


FIG. 9: Same as Fig. 8, but for electron scattering with real photon emission.

where $[c_\epsilon] \equiv i(4\pi)^{-2+\epsilon}\Gamma(1+\epsilon)$, and $p_-^\mu \equiv \bar{n} \cdot p n^\mu / 2$ is the large component of the momentum p^μ (similarly $p_-'^\mu$, is defined in terms of n'^μ and \bar{n}'^μ). This yields the one loop contribution to F_H^{bare} in Eq. (34).¹⁵

The soft contribution corresponds to the second diagram on the right hand side of Fig. 8. In dimensional regularization,

$$\delta F_S \gamma^\mu = -ie^2 \gamma^\mu \int \frac{d^d L}{(2\pi)^d} 4p \cdot p' \frac{1}{L^2 - \lambda^2} \frac{1}{2L \cdot p} \frac{1}{2L \cdot p'} = -ie^2 \gamma^\mu [c_\epsilon] \lambda^{-2\epsilon} \left[-\frac{2}{\epsilon} \log \frac{Q^2}{m^2} \right]. \quad (\text{E3})$$

Combined with the soft contribution to onshell wavefunction renormalization [Z_h in Eq. (A4)], this yields the one loop F_S^{bare} given by Eqs. (41) and (45).

The remaining contributions arise from momentum regions collinear to the final and initial electron momenta, shown as the final diagrams on the right hand side of Fig. 8. The

¹⁵ Recall that our definition of α_{bare} absorbs $e^{-\gamma_E \epsilon}$, whereas $[c_\epsilon]$ contains $\Gamma(1+\epsilon) = e^{-\gamma_E \epsilon}(1 + \epsilon^2 \pi^2 / 12 + \dots)$.

required basis of integrals is (the photon mass λ is irrelevant in this region and is taken to zero)

$$[I_c, I_c^\mu, I_c^{\mu\nu}] = \int \frac{d^d L}{(2\pi)^d} \frac{1}{L^2} \frac{1}{2L \cdot p_-} \frac{1}{L^2 + 2L \cdot p'} [1, L^\mu, L^\mu L^\nu]. \quad (\text{E4})$$

We expand

$$\begin{aligned} I_c &= [c_\epsilon] \frac{1}{Q^2} I^{(0)}, \\ I_c^\mu &= [c_\epsilon] \frac{1}{Q^2} \left[I_1^{(1)} p_-^\mu + I_2^{(1)} p'^\mu \right], \\ I_c^{\mu\nu} &= [c_\epsilon] \left[g^{\mu\nu} I_1^{(2)} + \frac{1}{Q^2} \left(I_2^{(2)} p_-^\mu p_-^\nu + I_3^{(2)} p'^\mu p'^\nu + I_4^{(2)} (p_-^\mu p'^\nu + p_-^\nu p'^\mu) \right) \right]. \end{aligned} \quad (\text{E5})$$

The necessary elementary integrals are

$$\begin{aligned} I^{(0)} &= \frac{m^{-2\epsilon}}{2\epsilon^2}, \\ I_2^{(1)} &= m^{-2\epsilon} \left(\frac{1}{\epsilon} + 2 \right), \end{aligned} \quad (\text{E6})$$

and we obtain

$$\delta F_J = -ie^2 [c_\epsilon] \left[2I^{(0)} + 2I_2^{(1)} + (p \leftrightarrow p') \right] = -ie^2 [c_\epsilon] m^{-2\epsilon} \left[\frac{2}{\epsilon^2} + \frac{4}{\epsilon} + 8 \right]. \quad (\text{E7})$$

Combined with the collinear contribution to onshell wavefunction renormalization [the difference of Z_Ψ and Z_h in Eq. (A4)], this yields the one loop F_J^{bare} given by Eq. (40) (recall that $F_R = 1$ at one loop order).

The sum of δF_H , δF_S and δF_J from Eqs. (E2), (E3) and (E7) reproduce the expression for δF at leading power in m^2/Q^2 which may be computed directly from Eq. (E1). The components of the factorization theorem (33) are thus identified with effective theory contributions represented by the diagrams of Fig. 8.

2. Real radiation

Consider now the case of real radiation at loop level. Begin with the interference between the diagram pictured in Fig. 9a, and the tree level photon emission diagrams from Fig. 1. The relevant integrals in the full theory evaluation are given by the first two terms of Eq. (D9), with four denominators. Let us focus in particular on the scalar integral,

$$I = \int \frac{d^d L}{(2\pi)^d} \frac{1}{L^2 - \lambda^2} \frac{1}{L^2 + 2L \cdot p} \frac{1}{L^2 + 2L \cdot p'} \frac{1}{L^2 + 2L \cdot (p' + k) + 2p' \cdot k}. \quad (\text{E8})$$

The soft photon contribution, represented by the first diagram on the RHS of Fig. 9a is

$$\begin{aligned}
I_s &= \int \frac{d^d L}{(2\pi)^d} \frac{1}{L^2 - \lambda^2} \frac{1}{2L \cdot p} \frac{1}{2L \cdot p'} \frac{1}{2(L+k) \cdot p'} \\
&= \frac{1}{Q^2} \frac{1}{2k \cdot p'} [c_\epsilon] \left[-2 \log^2 \frac{m^2}{Q^2} + 2 \log \frac{-2k \cdot p'}{\lambda Q} \log \frac{m^2}{Q^2} + \frac{\pi^2}{6} \right].
\end{aligned} \tag{E9}$$

The collinear contribution, represented by the second diagram on the RHS of Fig. 9a is

$$\begin{aligned}
I_c &= \int \frac{d^d L}{(2\pi)^d} \frac{1}{L^2} \frac{1}{2L_- \cdot p} \frac{1}{L^2 + 2L \cdot p'} \frac{1}{L^2 + 2L \cdot p' + 2k_+ \cdot (L + p')} \\
&= \frac{1}{2k \cdot p'} \int (dL) \frac{1}{L^2} \left(\frac{1}{n \cdot p \bar{n} \cdot (L + p')} - \frac{1}{n \cdot p \bar{n} \cdot L} \right) \\
&\quad \times \left(\frac{1}{L^2 + 2L \cdot p' + n \cdot k \bar{n} \cdot (L + p')} - \frac{1}{L^2 + 2L \cdot p'} \right) \\
&= \frac{1}{Q^2} \frac{1}{2k \cdot p'} [c_\epsilon] \frac{1}{\epsilon} J(1, 0, 0) = \frac{1}{Q^2} \frac{1}{2k \cdot p'} [c_\epsilon] (m^2 a)^{-2\epsilon} m^{2\epsilon} \left(\frac{1}{2\epsilon^2} + \frac{\pi^2}{6} \right),
\end{aligned} \tag{E10}$$

where we introduce the functions

$$J(r, s, t) = \int_0^1 dx x^s \left[\frac{1}{(1-x)^r} - \frac{1}{(-x)^r} \right] [x(1-x)m^2 a + x^2 m^2]^{t-\epsilon} - (x^2 m^2)^{t-\epsilon}. \tag{E11}$$

The presence of multiple low energy scales leads to a nontrivial subtraction in order to avoid double counting. The soft limit of the collinear integral is

$$I_c|_s = \int \frac{d^d L}{(2\pi)^d} \frac{1}{L^2} \frac{1}{2L_- \cdot p} \frac{1}{2L \cdot p'} \frac{1}{2(L+k_+) \cdot p'} = \frac{1}{Q^2} \frac{1}{2k \cdot p'} [c_\epsilon] (m^2 a)^{-2\epsilon} m^{2\epsilon} \left(-\frac{1}{2\epsilon^2} - \frac{\pi^2}{6} \right), \tag{E12}$$

so that accounting for the overlap, the collinear region gives vanishing contribution,

$$I_c - I_c|_s = 0. \tag{E13}$$

The remaining integrals may be treated similarly. For example, consider

$$I^\mu = \int \frac{d^d L}{(2\pi)^d} \frac{1}{L^2} \frac{1}{L^2 + 2L \cdot p} \frac{1}{L^2 + 2L \cdot p'} \frac{1}{L^2 + 2L \cdot (p' + k) + 2p' \cdot k} L^\mu. \tag{E14}$$

In the collinear region, we expand as

$$\begin{aligned}
I_c^\mu &= \int \frac{d^d L}{(2\pi)^d} \frac{1}{L^2} \frac{1}{2L_- \cdot p} \frac{1}{L^2 + 2L \cdot p'} \frac{1}{L^2 + 2L \cdot p' + 2k_+ \cdot (L + p')} L^\mu \\
&= \frac{1}{Q^2} \frac{1}{2k \cdot p'} [c_\epsilon] \left(I_1^{(1)} p'^\mu + I_2^{(1)} k_+^\mu \right),
\end{aligned} \tag{E15}$$

with

$$\begin{aligned} I_1^{(1)} &= -\frac{1}{\epsilon} J(1, 1, 0), \\ I_1^{(2)} &= -\frac{1}{\epsilon} K(1, 1, 0) + \frac{1}{m^2 a} \frac{1}{\epsilon(1-\epsilon)} J(2, 1, 0), \end{aligned} \quad (\text{E16})$$

where $J(n, m, p)$ is given above and

$$K(r, s, t) = \int_0^1 dx x^s \left[\frac{1}{(1-x)^r} - \frac{1}{(-x)^r} \right] (x(1-x)m^2 a + x^2 m^2)^{t-\epsilon}. \quad (\text{E17})$$

Explicit evaluation gives

$$I_1^{(1)} = -\text{Li}_2(1-a) + \frac{\pi^2}{6}. \quad (\text{E18})$$

Similarly, consider

$$I^{\mu\nu} = \int \frac{d^d L}{(2\pi)^d} \frac{1}{L^2} \frac{1}{L^2 + 2L \cdot p} \frac{1}{L^2 + 2L \cdot p'} \frac{1}{L^2 + 2L \cdot (p' + k) + 2p' \cdot k} L^\mu L^\nu. \quad (\text{E19})$$

In the collinear region, we expand as

$$\begin{aligned} I_c^{\mu\nu} &= \int \frac{d^d L}{(2\pi)^d} \frac{1}{L^2} \frac{1}{2L_- \cdot p} \frac{1}{L^2 + 2L \cdot p'} \frac{1}{L^2 + 2L \cdot p' + 2k_+ \cdot (L + p')} L^\mu L^\nu \\ &= \frac{1}{Q^2} \frac{1}{2k \cdot p'} [c_\epsilon] \left(I_1^{(2)} g^{\mu\nu} + I_2^{(2)} p'^\mu p'^\nu + I_3^{(2)} (p'^\mu k_+^\nu + k_+^\mu p'^\nu) + I_4^{(2)} k_+^\mu k_+^\nu \right), \end{aligned} \quad (\text{E20})$$

with

$$\begin{aligned} I_1^{(2)} &= \frac{1}{2\epsilon(1-\epsilon)} J(1, 0, 1), \\ I_2^{(2)} &= \frac{1}{\epsilon} J(1, 2, 0), \\ I_3^{(2)} &= \frac{1}{\epsilon} K(1, 2, 0) - \frac{1}{m^2 a} \frac{1}{\epsilon(1-\epsilon)} J(2, 1, 1), \\ I_4^{(2)} &= \frac{1}{\epsilon} K(1, 2, 0) - \frac{2}{m^2 a} \frac{1}{\epsilon(1-\epsilon)} K(2, 1, 1), \\ I_4^{(2)} &= \frac{1}{\epsilon} K(1, 2, 0) - \frac{2}{m^2 a} \frac{1}{\epsilon(1-\epsilon)} K(2, 1, 1) + \frac{2}{(m^2 a)^2} \frac{1}{\epsilon(1-\epsilon)(2-\epsilon)} J(3, 0, 2). \end{aligned} \quad (\text{E21})$$

The relevant integrals are, explicitly,

$$I_2^{(2)} = \text{Li}_2(1-a) + \frac{a}{a-1} \log a - \frac{\pi^2}{6}. \quad (\text{E22})$$

Note that there are no leading-power soft contributions corresponding to the full theory diagram in Fig. 9 involving the photon loop momentum L^μ in the numerator.

Using these integrals, an explicit evaluation of the diagram in Fig. 9a yields

$$\begin{aligned}
& \left(\sum |\mathcal{M}_1|^2 \right)_{\text{Fig.9a, collinear}} \\
&= 2\text{Re} \sum \left(\text{Diagram 1} + \text{Diagram 2} \right)^* \left(\text{Diagram 3} + \text{Diagram 4} \right) \\
&= e^2 \sum |\mathcal{M}_0|^2 \frac{\alpha}{4\pi} \frac{2v \cdot v'}{v \cdot k v' \cdot k} \text{Re} \left[4I_1^{(1)} + 2I_2^{(2)} + (a \rightarrow b) \right] \\
&= e^2 \sum |\mathcal{M}_0|^2 \frac{\alpha}{4\pi} \frac{2v \cdot v'}{v \cdot k v' \cdot k} \text{Re} \left[-2\text{Li}_2(1-a) + \frac{\pi^2}{3} - \frac{2a}{1-a} \log a + (a \rightarrow b) \right]. \quad (\text{E23})
\end{aligned}$$

Similarly, (extracting the overall factor $\mathcal{C} = e^2 \sum |\mathcal{M}_0|^2 e_{\text{bare}}^2 (4\pi)^{-2+\epsilon} \Gamma(1+\epsilon) m^{-2\epsilon}$, and real part implied),

$$\begin{aligned}
\mathcal{C}^{-1} \left(\sum |\mathcal{M}_1|^2 \right)_{\text{Fig.9b, collinear}} &= \left[\frac{1}{(v \cdot k)^2} + \frac{1}{(v' \cdot k)^2} - \frac{2v \cdot v'}{v \cdot k v' \cdot k} \right] \left[-\frac{4}{\epsilon^2} - \frac{8}{\epsilon} \right] \\
&+ \left[\frac{1}{(v \cdot k)^2} + \frac{1}{(v' \cdot k)^2} \right] (-16) \\
&+ \frac{2v \cdot v'}{v \cdot k v' \cdot k} \text{Re} \left[2\text{Li}_2(1-a) - \frac{\pi^2}{3} + \frac{2a}{1-a} \log a + 8 + (a \rightarrow b) \right], \\
\mathcal{C}^{-1} \left(\sum |\mathcal{M}_1|^2 \right)_{\text{Fig.9c, collinear}} &= \left[\frac{1}{(v \cdot k)^2} + \frac{1}{(v' \cdot k)^2} - \frac{2v \cdot v'}{v \cdot k v' \cdot k} \right] \left(-\frac{6}{\epsilon} \right) \\
&+ \left[\frac{1}{(v \cdot k)^2} + \frac{1}{(v' \cdot k)^2} \right] (-8) + \frac{2v \cdot v'}{v \cdot k v' \cdot k} \left[-\frac{a(5a-4)}{(a-1)^2} \log a + \frac{5a-4}{a-1} + (a \rightarrow b) \right], \\
\mathcal{C}^{-1} \left(\sum |\mathcal{M}_1|^2 \right)_{\text{Fig.9d, collinear}} &= -\mathcal{C}^{-1} \left(\sum |\mathcal{M}_1|^2 \right)_{\text{Fig.9c, collinear}}, \\
\mathcal{C}^{-1} \left(\sum |\mathcal{M}_1|^2 \right)_{\text{Fig.9e, collinear}} &= \left[\frac{1}{(v \cdot k)^2} + \frac{1}{(v' \cdot k)^2} - \frac{2v \cdot v'}{v \cdot k v' \cdot k} \right] \left(\frac{6}{\epsilon} + 8 \right). \quad (\text{E24})
\end{aligned}$$

Summing contributions, we find

$$\begin{aligned}
\left(\sum |\mathcal{M}_1|^2 \right)_{\text{collinear}} &= e^2 \sum |\mathcal{M}_0|^2 \frac{\alpha}{4\pi} \left(\frac{m^2}{\mu^2} \right)^{-\epsilon} \left[\frac{1}{(v \cdot k)^2} + \frac{1}{(v' \cdot k)^2} - \frac{2v \cdot v'}{v \cdot k v' \cdot k} \right] \\
&\times \left[-\frac{4}{\epsilon^2} - \frac{2}{\epsilon} - 8 \right] \quad (\text{E25})
\end{aligned}$$

For the soft contributions,

$$\begin{aligned}
\mathcal{C}^{-1} \left(\sum |\mathcal{M}_1|^2 \right)_{\text{Fig.9a, soft}} &= \left[\frac{1}{(v \cdot k)^2} - \frac{v \cdot v'}{v \cdot k v' \cdot k} \right] \left[-4L^2 + 8 \log \frac{ma}{\lambda} L - \frac{2\pi^2}{3} \right] \\
&+ \left[\frac{1}{(v' \cdot k)^2} - \frac{v \cdot v'}{v \cdot k v' \cdot k} \right] \left[-4L^2 + 8 \log \frac{mb}{\lambda} L - \frac{2\pi^2}{3} \right],
\end{aligned}$$

$$\begin{aligned}
\mathcal{C}^{-1}(\sum |\mathcal{M}_1|^2)_{\text{Fig.9b, soft}} &= \left[\frac{1}{(v \cdot k)^2} - \frac{v \cdot v'}{v \cdot k v' \cdot k} \right] \left[\frac{4}{\epsilon} L - 8L \log a + 4L^2 + \frac{2\pi^2}{3} \right] \\
&\quad + \left[\frac{1}{(v' \cdot k)^2} - \frac{v \cdot v'}{v \cdot k v' \cdot k} \right] \left[\frac{4}{\epsilon} L - 8L \log b + 4L^2 + \frac{2\pi^2}{3} \right], \\
\mathcal{C}^{-1}(\sum |\mathcal{M}_1|^2)_{\text{Fig.9c, soft}} &= \left[\frac{1}{(v \cdot k)^2} - \frac{v \cdot v'}{v \cdot k v' \cdot k} \right] \left[\frac{4}{\epsilon} - 8 \log a + 8 \right] \\
&\quad + \left[\frac{1}{(v' \cdot k)^2} - \frac{v \cdot v'}{v \cdot k v' \cdot k} \right] \left[\frac{4}{\epsilon} - 8 \log b + 8 \right], \\
\mathcal{C}^{-1}(\sum |\mathcal{M}_1|^2)_{\text{Fig.9d, soft}} &= \left[\frac{1}{(v \cdot k)^2} - \frac{v \cdot v'}{v \cdot k v' \cdot k} \right] \left[-\frac{4}{\epsilon} - 8 + 8 \log a \right] \\
&\quad + \left[\frac{1}{(v' \cdot k)^2} - \frac{v \cdot v'}{v \cdot k v' \cdot k} \right] \left[-\frac{4}{\epsilon} - 8 + 8 \log b \right], \\
\mathcal{C}^{-1}(\sum |\mathcal{M}_1|^2)_{\text{Fig.9e, soft}} &= \left[\frac{1}{(v \cdot k)^2} + \frac{1}{(v' \cdot k)^2} - \frac{2v \cdot v'}{v \cdot k v' \cdot k} \right] \left[-\frac{4}{\epsilon} + 8 \log \frac{\lambda}{m} \right]. \quad (\text{E26})
\end{aligned}$$

Summing contributions,

$$\begin{aligned}
(\sum |\mathcal{M}_1|^2)_{\text{soft}} &= e^2 \sum |\mathcal{M}_0|^2 \frac{\alpha}{4\pi} \left(\frac{m^2}{\mu^2} \right)^{-\epsilon} \left[\frac{1}{(v \cdot k)^2} + \frac{1}{(v' \cdot k)^2} - \frac{2v \cdot v'}{v \cdot k v' \cdot k} \right] \\
&\quad \times \left[\frac{1}{\epsilon} (4L - 4) - 8(L - 1) \log \frac{\lambda}{m} \right]. \quad (\text{E27})
\end{aligned}$$

For the hard contribution, only Fig. 9b contributes,

$$\begin{aligned}
(\sum |\mathcal{M}_1|^2)_{\text{hard}} &= e^2 \sum |\mathcal{M}_0|^2 \frac{\alpha}{4\pi} \left(\frac{m^2}{\mu^2} \right)^{-\epsilon} \left[\frac{1}{(v \cdot k)^2} + \frac{1}{(v' \cdot k)^2} - \frac{2v \cdot v'}{v \cdot k v' \cdot k} \right] \\
&\quad \times \left[\frac{4}{\epsilon^2} + \frac{1}{\epsilon} (-4L + 6) + 2L^2 - 6L + 16 - \frac{2\pi^2}{3} \right]. \quad (\text{E28})
\end{aligned}$$

The contribution from the analog of Fig. 9 with photon emitted from the initial state electron results in the same expressions with $a \leftrightarrow b$. The sum of hard, collinear and soft contributions is identical at leading power to the full theory evaluation above.

This analysis shows that individual diagrams contain nonvanishing contributions from soft photons emitted interior to collinear photon loops. As discussed around Eq. (D8), the presence of multiple momentum modes contributing at leading power to the real-photon phase space integration complicates a simple factorization argument. Nonetheless, an explicit evaluation reveals that factorization holds in the sum over diagrams, at least through one loop order, consistent with the direct evaluation (D11). This leads to the simple expres-

sion (31), as required by the factorization formula (33).

-
- [1] R. Pohl *et al.*, Nature **466**, 213 (2010).
 - [2] P. J. Mohr, B. N. Taylor and D. B. Newell, Rev. Mod. Phys. **84**, 1527 (2012) [arXiv:1203.5425 [physics.atom-ph]].
 - [3] I. Sick, Phys. Lett. B **576**, 62 (2003) [nucl-ex/0310008].
 - [4] J. C. Bernauer *et al.* [A1 Collaboration], Phys. Rev. Lett. **105**, 242001 (2010) [arXiv:1007.5076 [nucl-ex]].
 - [5] X. Zhan, K. Allada, D. S. Armstrong, J. Arrington, W. Bertozzi, W. Boeglin, J.-P. Chen and K. Chirapatpimol *et al.*, Phys. Lett. B **705**, 59 (2011) [arXiv:1102.0318 [nucl-ex]].
 - [6] G. Lee, J. R. Arrington and R. J. Hill, Phys. Rev. D **92**, no. 1, 013013 (2015) [arXiv:1505.01489 [hep-ph]].
 - [7] J. C. Bernauer *et al.* [A1 Collaboration], Phys. Rev. C **90**, no. 1, 015206 (2014) [arXiv:1307.6227 [nucl-ex]].
 - [8] R. J. Hill and G. Paz, Phys. Rev. D **82**, 113005 (2010) [arXiv:1008.4619 [hep-ph]].
 - [9] Z. Epstein, G. Paz and J. Roy, Phys. Rev. D **90**, no. 7, 074027 (2014) [arXiv:1407.5683 [hep-ph]].
 - [10] D. R. Yennie, S. C. Frautschi and H. Suura, Annals Phys. **13**, 379 (1961).
 - [11] M. Neubert, Phys. Rept. **245**, 259 (1994) [hep-ph/9306320].
 - [12] A. V. Manohar and M. B. Wise, Camb. Monogr. Part. Phys. Nucl. Phys. Cosmol. **10**, 1 (2000).
 - [13] W. E. Caswell and G. P. Lepage, Phys. Lett. B **167**, 437 (1986).
 - [14] J. Heinonen, R. J. Hill and M. P. Solon, Phys. Rev. D **86**, 094020 (2012) [arXiv:1208.0601 [hep-ph]].
 - [15] M. Neubert, Phys. Rev. D **46**, 2212 (1992).
 - [16] G. P. Korchemsky and A. V. Radyushkin, Nucl. Phys. B **283**, 342 (1987).
 - [17] W. Kilian, P. Manakos and T. Mannel, Phys. Rev. D **48**, 1321 (1993).
 - [18] C. W. Bauer, S. Fleming and M. E. Luke, Phys. Rev. D **63**, 014006 (2000) [hep-ph/0005275].
 - [19] C. W. Bauer, S. Fleming, D. Pirjol and I. W. Stewart, Phys. Rev. D **63**, 114020 (2001) [hep-ph/0011336].
 - [20] C. W. Bauer and I. W. Stewart, Phys. Lett. B **516**, 134 (2001) [hep-ph/0107001].

- [21] C. W. Bauer, D. Pirjol and I. W. Stewart, Phys. Rev. D **65**, 054022 (2002) [hep-ph/0109045].
- [22] J. Chay and C. Kim, Phys. Rev. D **65**, 114016 (2002) [hep-ph/0201197].
- [23] M. Beneke, A. P. Chapovsky, M. Diehl and T. Feldmann, Nucl. Phys. B **643**, 431 (2002) [hep-ph/0206152].
- [24] R. J. Hill and M. Neubert, Nucl. Phys. B **657**, 229 (2003) [hep-ph/0211018].
- [25] For a review and further references, see: T. Becher, A. Broggio and A. Ferroglia, arXiv:1410.1892 [hep-ph].
- [26] G. J. H. Burgers, Phys. Lett. B **164**, 167 (1985).
- [27] B. A. Kniehl, Phys. Lett. B **237**, 127 (1990).
- [28] P. Mastrolia and E. Remiddi, Nucl. Phys. B **664**, 341 (2003) [hep-ph/0302162].
- [29] S. Moch, J. A. M. Vermaseren and A. Vogt, JHEP **0508**, 049 (2005) [hep-ph/0507039].
- [30] T. Gehrmann, T. Huber and D. Maitre, Phys. Lett. B **622**, 295 (2005) [hep-ph/0507061].
- [31] T. Gehrmann, private communication.
- [32] A. H. Hoang, J. H. Kuhn and T. Teubner, Nucl. Phys. B **452**, 173 (1995) [hep-ph/9505262].
- [33] W. Bernreuther, R. Bonciani, T. Gehrmann, R. Heinesch, T. Leineweber, P. Mastrolia and E. Remiddi, Nucl. Phys. B **706**, 245 (2005) [hep-ph/0406046].
- [34] T. Becher and K. Melnikov, JHEP **0706**, 084 (2007) [arXiv:0704.3582 [hep-ph]].
- [35] D. J. Broadhurst and A. G. Grozin, Phys. Rev. D **52**, 4082 (1995) [hep-ph/9410240].
- [36] J. y. Chiu, F. Golf, R. Kelley and A. V. Manohar, Phys. Rev. D **77**, 053004 (2008) doi:10.1103/PhysRevD.77.053004 [arXiv:0712.0396 [hep-ph]].
- [37] T. Becher and M. Neubert, Eur. Phys. J. C **71**, 1665 (2011) doi:10.1140/epjc/s10052-011-1665-7 [arXiv:1007.4005 [hep-ph]].
- [38] J. Y. Chiu, A. Jain, D. Neill and I. Z. Rothstein, JHEP **1205**, 084 (2012) doi:10.1007/JHEP05(2012)084 [arXiv:1202.0814 [hep-ph]].
- [39] A. B. Arbuzov and T. V. Kopylova, Eur. Phys. J. C **75**, no. 12, 603 (2015) [arXiv:1510.06497 [hep-ph]].
- [40] L. C. Maximon and J. A. Tjon, Phys. Rev. C **62**, 054320 (2000) [nucl-th/0002058].
- [41] D. Rimal *et al.* [CLAS Collaboration], arXiv:1603.00315 [nucl-ex].
- [42] P. G. Blunden, W. Melnitchouk and J. A. Tjon, Phys. Rev. Lett. **91**, 142304 (2003) [nucl-th/0306076]. J. Arrington, Phys. Rev. C **69**, 022201 (2004) [nucl-ex/0309011]. Y. C. Chen, A. Afanasev, S. J. Brodsky, C. E. Carlson and M. Vanderhaeghen, Phys. Rev. Lett. **93**,

- 122301 (2004) [hep-ph/0403058]. A. V. Afanasev and C. E. Carlson, Phys. Rev. Lett. **94**, 212301 (2005) [hep-ph/0502128]. A. V. Afanasev, S. J. Brodsky, C. E. Carlson, Y. C. Chen and M. Vanderhaeghen, Phys. Rev. D **72**, 013008 (2005) [hep-ph/0502013]. P. G. Blunden, W. Melnitchouk and J. A. Tjon, Phys. Rev. C **72**, 034612 (2005) [nucl-th/0506039]. S. Kondratyuk and P. G. Blunden, Nucl. Phys. A **778**, 44 (2006) [nucl-th/0601063]. M. A. Belushkin, H.-W. Hammer and U.-G. Meissner, Phys. Rev. C **75**, 035202 (2007) [hep-ph/0608337]. S. Kondratyuk and P. G. Blunden, Phys. Rev. C **75**, 038201 (2007) [nucl-th/0701003]. J. Arrington, W. Melnitchouk and J. A. Tjon, Phys. Rev. C **76**, 035205 (2007) [arXiv:0707.1861 [nucl-ex]]. D. Borisjuk and A. Kobushkin, Phys. Rev. C **78**, 025208 (2008) [arXiv:0804.4128 [nucl-th]]. D. Borisjuk and A. Kobushkin, Phys. Rev. C **86**, 055204 (2012) [arXiv:1206.0155 [hep-ph]]. D. Borisjuk and A. Kobushkin, Phys. Rev. C **89**, no. 2, 025204 (2014) [arXiv:1306.4951 [hep-ph]]. H. Q. Zhou and S. N. Yang, Eur. Phys. J. A **51**, no. 8, 105 (2015) [arXiv:1407.2711 [nucl-th]]. O. Tomalak and M. Vanderhaeghen, Eur. Phys. J. A **51**, no. 2, 24 (2015) [arXiv:1408.5330 [hep-ph]]. I. T. Lorenz, U. G. Meiner, H.-W. Hammer and Y.-B. Dong, Phys. Rev. D **91**, no. 1, 014023 (2015) [arXiv:1411.1704 [hep-ph]]. S. P. Dye, M. Gonderinger and G. Paz, arXiv:1602.07770 [hep-ph].
- [43] For reviews and further references, see: C. E. Carlson and M. Vanderhaeghen, Ann. Rev. Nucl. Part. Sci. **57**, 171 (2007) [hep-ph/0701272 [HEP-PH]]. J. Arrington, P. G. Blunden and W. Melnitchouk, Prog. Part. Nucl. Phys. **66**, 782 (2011) [arXiv:1105.0951 [nucl-th]].
- [44] M. Vanderhaeghen, J. M. Friedrich, D. Lhuillier, D. Marchand, L. Van Hoorebeke and J. Van de Wiele, Phys. Rev. C **62**, 025501 (2000) [hep-ph/0001100].
- [45] W. A. McKinley and H. Feshbach, Phys. Rev. **74**, 1759 (1948).
- [46] I. Sick, Prog. Part. Nucl. Phys. **67**, 473 (2012).
- [47] J. R. Arrington, R. J. Hill, G. Lee and Z. Ye, *in preparation*.
- [48] S. Actis *et al.* [Working Group on Radiative Corrections and Monte Carlo Generators for Low Energies Collaboration], Eur. Phys. J. C **66**, 585 (2010) [arXiv:0912.0749 [hep-ph]].
- [49] F. Jegerlehner, Nuovo Cim. C **034S1**, 31 (2011) [arXiv:1107.4683 [hep-ph]].
- [50] A. V. Gramolin, V. S. Fadin, A. L. Feldman, R. E. Gerasimov, D. M. Nikolenko, I. A. Rachek and D. K. Toporkov, J. Phys. G **41**, no. 11, 115001 (2014) [arXiv:1401.2959 [nucl-ex]].
- [51] I. Akushevich, H. Gao, A. Ilyichev and M. Meziane, Eur. Phys. J. A **51**, no. 1, 1 (2015).
- [52] A. V. Gramolin and D. M. Nikolenko, arXiv:1603.06920 [nucl-ex].

- [53] M. Day and K. S. McFarland, Phys. Rev. D **86**, 053003 (2012).
- [54] J. P. Lees *et al.* [BaBar Collaboration], Phys. Rev. D **92**, no. 7, 072015 (2015) [arXiv:1508.04008 [hep-ex]].
- [55] J. Benesch *et al.* [MOLLER Collaboration], arXiv:1411.4088 [nucl-ex].
- [56] A. G. Aleksejevs, S. G. Barkanova, Y. M. Bystritskiy, E. A. Kuraev, A. N. Ilyichev and V. A. Zykunov, arXiv:1202.0378 [hep-ph].
- [57] A. G. Aleksejevs, S. G. Barkanova, Y. M. Bystritskiy, E. A. Kuraev and V. A. Zykunov, Phys. Part. Nucl. Lett. **12**, no. 5, 645 (2015) doi:10.1134/S1547477115050039 [arXiv:1504.03560 [hep-ph]].
- [58] T. Becher, R. J. Hill, B. O. Lange and M. Neubert, Phys. Rev. D **69**, 034013 (2004) [hep-ph/0309227].
- [59] T. Becher and M. Neubert, JHEP **0906**, 081 (2009) Erratum: [JHEP **1311**, 024 (2013)] [arXiv:0903.1126 [hep-ph]].
- [60] T. Becher and M. Neubert, Phys. Rev. D **79**, 125004 (2009) Erratum: [Phys. Rev. D **80**, 109901 (2009)] [arXiv:0904.1021 [hep-ph]].
- [61] M. Beneke, P. Falgari and C. Schwinn, Nucl. Phys. B **828**, 69 (2010) [arXiv:0907.1443 [hep-ph]].
- [62] R. J. Hill and G. Paz, Phys. Rev. Lett. **107**, 160402 (2011) [arXiv:1103.4617 [hep-ph]].
- [63] K. Pachucki, Phys. Rev. A **60**, 3593 (1999).
- [64] G. 't Hooft and M. J. G. Veltman, Nucl. Phys. B **153**, 365 (1979).